

Approximate Vanishing Ideal Computations at Scale

Elias Wirth

WIRTH@ZIB.DE

*Institute of Mathematics & AI in Society, Science, and Technology
Technische Universität Berlin & Zuse Institute Berlin
Berlin, Germany*

Hiroshi Kera

KERA.HIROSHI@GMAIL.COM

*Graduate School of Engineering
Chiba University
Chiba, Japan*

Sebastian Pokutta

POKUTTA@ZIB.DE

*Institute of Mathematics & AI in Society, Science, and Technology
Technische Universität Berlin & Zuse Institute Berlin
Berlin, Germany*

Abstract

The approximate vanishing ideal of a set of points $X = \{\mathbf{x}_1, \dots, \mathbf{x}_m\} \subseteq [0, 1]^n$ is the set of polynomials that approximately evaluate to 0 over all points $\mathbf{x} \in X$ and admits an efficient representation by a finite set of polynomials called generators. Algorithms that construct this set of generators are extensively studied but ultimately find little practical application because their computational complexities are thought to be superlinear in the number of samples m . In this paper, we focus on scaling up the *Oracle Approximate Vanishing Ideal algorithm* (OAVI), one of the most powerful of these methods. We prove that the computational complexity of OAVI is not superlinear but linear in the number of samples m and polynomial in the number of features n , making OAVI an attractive preprocessing technique for large-scale machine learning. To further accelerate OAVI’s training time, we propose two changes: First, as the name suggests, OAVI makes repeated oracle calls to convex solvers throughout its execution. By replacing the *Pairwise Conditional Gradients algorithm* (PCG), one of the standard solvers used in OAVI, with the faster *Blended Pairwise Conditional Gradients algorithm* (BPCG), we illustrate how OAVI directly benefits from advancements in the study of convex solvers. Second, we propose *Inverse Hessian Boosting* (IHB): IHB exploits the fact that OAVI repeatedly solves quadratic convex optimization problems that differ only by very little and whose solutions can be written in closed form using inverse Hessian information. By efficiently updating the inverse of the Hessian matrix, the convex optimization problems can be solved almost instantly, accelerating OAVI’s training time by up to multiple orders of magnitude. We complement our theoretical analysis with extensive numerical experiments on data sets whose sample numbers are in the millions.

1. Introduction

High-quality features are essential for the success of machine learning algorithms (Guyon and Elisseeff, 2003) and as a consequence, feature transformation and selection algorithms are an important area of research (Kusiak, 2001; Stone, 2004; Van Der Maaten et al., 2009; Abdi and Williams, 2010; Paul et al., 2021; Pokutta et al., 2020; Manikandan and Abirami, 2021; Carderera et al., 2021). A recently popularized technique for extracting non-linear features from data is the concept of the vanishing ideal (Heldt et al., 2009; Livni et al., 2013), which lies at the intersection of machine learning and computer algebra. Unlike conventional machine learning, which relies on the manifold assumption, vanishing ideal computations are based on the algebraic set¹ assumption, for which powerful theoretical guarantees are known (Vidal et al., 2005; Livni et al., 2013; Globerson et al., 2017). The core concept of vanishing ideal computations is that any data set

1. A set $X \subseteq \mathbb{R}^n$ is *algebraic* if there exists a finite set of polynomials \mathcal{G} , such that X is the set of the common roots of \mathcal{G} .

$X = \{\mathbf{x}_1, \dots, \mathbf{x}_m\} \subseteq \mathbb{R}^n$ can be described by its *vanishing ideal*,

$$\mathcal{I}_X = \{g \in \mathcal{P} \mid g(\mathbf{x}) = 0 \text{ for all } \mathbf{x} \in X\},$$

where \mathcal{P} is the polynomial ring over \mathbb{R} in n variables.² Despite \mathcal{I}_X containing infinitely many polynomials, there exists a finite number of *generators* of \mathcal{I}_X , $g_1, \dots, g_k \in \mathcal{I}_X$ with $k \in \mathbb{N}$, such that any polynomial $h \in \mathcal{I}_X$ can be written as

$$h = \sum_{i=1}^k g_i h_i,$$

where $h_i \in \mathcal{P}$ for all $i \in \{1, \dots, k\}$ (Cox et al., 2013). Thus, the generators share any sample $\mathbf{x} \in X$ as a common root, capture the nonlinear structure of the data, and succinctly represent the vanishing ideal \mathcal{I}_X . In practice, due to noise in the data set, we are interested in constructing generators of the *approximate vanishing ideal*, the set of polynomials that approximately evaluate to 0 for all $\mathbf{x} \in X$ and whose leading term coefficient is 1, see Definition 2.2.

Constructed generators can be used to transform the features of the data set $X = \{\mathbf{x}_1, \dots, \mathbf{x}_m\} \subseteq [0, 1]^n$ such that the data becomes linearly separable (Livni et al., 2013).³ Consider, for example, a binary classification task where the samples of the data set $X \subseteq \mathbb{R}^n$ either belong to class 1 or class 2. Letting X^1, X^2 denote the subsets of samples corresponding to class 1 and 2, we construct sets of generators $\mathcal{G}^1, \mathcal{G}^2$ of the approximate vanishing ideals of X^1 and X^2 , respectively, by applying OAVI twice, once to X^1 and once to X^2 . Then, under the assumption that X^1 and X^2 are disjoint algebraic sets, polynomials $g \in \mathcal{G}^1$ and $h \in \mathcal{G}^2$ satisfy

$$g(\mathbf{x}) = \begin{cases} \approx 0, & \mathbf{x} \in X^1 \\ \neq 0, & \mathbf{x} \in X^2 \end{cases} \quad \text{and} \quad h(\mathbf{x}) = \begin{cases} \approx 0, & \mathbf{x} \in X^2 \\ \neq 0, & \mathbf{x} \in X^1 \end{cases},$$

respectively. Under mild assumptions, evaluating all generators in $\mathcal{G} = \mathcal{G}^1 \cup \mathcal{G}^2$ over the entire data set X and taking the absolute values maps the data into a feature space in which the two classes are linearly separable. Training a linear classifier such as a linear kernel *Support Vector Machine* (SVM) (Suykens and Vandewalle, 1999) on the feature-transformed data set results in excellent classification accuracy.

Various algorithms for the construction of generators of the approximate vanishing ideal exist (Heldt et al., 2009; Fassino, 2010; Limbeck, 2013; Livni et al., 2013; Király et al., 2014; Iraj and Chitsaz, 2017; Kera and Hasegawa, 2020; Kera, 2021), but among them, the *Oracle Approximate Vanishing Ideal algorithm* (OAVI) (Wirth and Pokutta, 2022) enjoys some of the strongest theoretical guarantees. By reformulating the construction of generators as constrained convex optimization problems, a variant of OAVI constructs generators of the approximate vanishing ideal via oracle calls to the *Frank-Wolfe algorithm* (Frank and Wolfe, 1956), a.k.a. the *Conditional Gradients algorithm* (CG) (Levitin and Polyak, 1966). More specifically, CGAVI (OAVI with CG as a solver) exploits the sparsity-inducing properties of the *Pairwise Conditional Gradients algorithm* (PCG) (Guélat and Marcotte, 1986; Lacoste-Julien and Jaggi, 2015), which results in the construction of few and sparse generators and, thus, a robust and interpretable feature transformation corresponding to the constructed generators. Furthermore, generators constructed with CGAVI vanish on out-sample data⁴ and the combined approach of transforming features with CGAVI for a subsequently applied linear kernel SVM inherits the generalization bound of the SVM. Despite OAVI’s various appealing properties, the computational complexities of OAVI and related methods for the construction of generators of the approximate vanishing ideal are superlinear in the number of samples m . With training times, in particular, that increase cubically with m , OAVI and related methods have yet to be used in large-scale machine learning problems.

In this paper, we improve OAVI’s computational complexity and time complexity, in particular, and present modifications to the algorithm that turn OAVI into a fast and data-driven feature transformation technique that can be applied to data sets consisting of multiple millions of samples.

2. A set of polynomials $\mathcal{I} \subseteq \mathcal{P}$ is an *ideal* if it is a subgroup with respect to addition and if for all $g \in \mathcal{I}$ and $h \in \mathcal{P}$, it holds that $g \cdot h \in \mathcal{I}$.

3. A detailed overview of the machine learning pipeline associated with OAVI is given in Section 3.2 and Algorithm 2, specifically.

4. Out-sample data is distributed according to the same distribution as the training data but is not used during training.

1.1 Contributions

Our contributions are five-fold:

Linear computational complexity in m . Up until now, the analysis of computational complexities of OAVI and related methods relied on the assumption that generators need to vanish exactly, which gave an overly pessimistic estimation of the computational cost. For OAVI, we develop a new analysis that works with the more practical setting, that is, in case the generators only have to vanish approximately, and prove that the computational complexity of OAVI is not superlinear but linear in the number of samples m and polynomial in the number of features n .

Solver improvements improve OAVI. OAVI repeatedly calls a solver of quadratic convex optimization problems to construct generators. By replacing PCG with the faster *Blended Pairwise Conditional Gradients algorithm* (BPCG) (Tsuiji et al., 2021), we improve the dependence of the time complexity of OAVI on the number of features n in the data set by an exponential factor. We thus illustrate how advances in the running times of convex solvers lead to advances in the training time of OAVI.

Inverse Hessian Boosting (IHB). Throughout its execution, OAVI solves a series of quadratic convex optimization problems that differ from each other only slightly. We propose *Inverse Hessian Boosting* (IHB), a technique that exploits this fact by efficiently maintaining and updating the inverse of the Hessian of the quadratic convex optimization problems solved throughout OAVI’s execution. Since the optimal solution of a quadratic convex optimization problem can be written in closed form using the inverse of the Hessian matrix, the training time of OAVI is reduced tremendously, leading to empirical speed-ups of up to multiple orders of magnitude.

Data-driven ordering. As a monomial-aware approach, OAVI relies on a term ordering and is not fully data-driven, that is, OAVI’s output depends on the order of the features of the data set X . We propose a simple scheme for ordering the features of the data set X to make OAVI and other monomial-aware algorithms fully data-driven in that their outputs no longer depend on the order of the features of the data set X .

Large-scale numerical experiments. We perform extensive numerical experiments on data sets of up to two million samples, highlighting that OAVI is an excellent large-scale feature transformation method for a subsequently applied linear classifier.

In summary, with the theoretical results for and modifications of OAVI introduced in this paper, OAVI becomes a data-driven algorithm that quickly constructs few and sparse generators of the approximate vanishing ideal for massive data sets and enjoys several generalization bounds (when combined with a subsequently applied linear kernel SVM).

1.2 Related work

The *Buchberger-Möller algorithm* was the first method for constructing generators of the vanishing ideal (Möller and Buchberger, 1982). Since the algorithm constructs vanishing and not approximately vanishing polynomials, it is highly susceptible to noise. This shortcoming was subsequently addressed by Heldt et al. (2009) with the introduction of the *Approximate Vanishing Ideal algorithm* (AVI), which constructs generators of the approximate vanishing ideal in a stable manner. AVI was further refined by Fassino (2010) and Limbeck (2013). The latter also introduced two algorithms that construct generators term by term instead of degree-wise such as AVI, the *Approximate Buchberger-Möller algorithm* (ABM) and the *Border Bases Approximate Buchberger-Möller algorithm*, which is similar to OAVI. OAVI, ABM, and AVI are monomial-aware, that is, they require an explicit ordering of terms and construct generators as linear combinations of monomials. The dependence on a term ordering is an unattractive property: It implies that changing the order of the features changes the outputs of the algorithms, making the algorithms not fully data-driven.

Monomial-agnostic approaches such as *Vanishing Component Analysis* (VCA) (Livni et al., 2013) do not suffer from this shortcoming. Instead of relying on a term ordering and constructing generators as linear combinations of monomials, they construct generators as linear combinations of polynomials, making monomial-agnostic algorithms agnostic towards the ordering of the features of the data set, that is, fully data-driven. VCA has been applied to hand posture recognition, solution selection using genetic programming, principal variety analysis for nonlinear data modeling, and independent signal estimation for blind source separation (Zhao and Song, 2014; Kera and Iba, 2016; Iraj and Chitsaz, 2017; Wang and Ohtsuki, 2018) and the connection to kernels has also been studied (Király et al., 2014; Hou et al., 2016). However, foregoing the term ordering also comes with its disadvantages: VCA sometimes constructs multiple orders of magnitudes more (unnecessary) generators than monomial-aware algorithms (Wirth and Pokutta, 2022). Furthermore, VCA is susceptible to the *spurious vanishing problem*: In VCA, polynomials that do not capture the nonlinear structure of the data but whose coefficient vector entries are small become generators and conversely, polynomials that capture the data well but whose coefficient vector entries are large get treated as non-vanishing. Recently, Kera and Hasegawa (2019; 2020; 2021) managed to mitigate the spurious vanishing problem for VCA to some extent.⁵

1.3 Outline

Section 2 contains the preliminaries. In Section 3, we give a brief overview of OAVI and the associated machine learning pipeline. In Section 4, we improve the scalability of OAVI. In Section 5, we propose a simple scheme to make monomial-aware algorithms data-driven. In Section 6, we present the numerical experiments. In Section 7, we summarize the impact of our results.

2. Preliminaries

We recall notations and the theoretical background necessary to introduce OAVI.

2.1 Notations

Throughout, let $\ell, k, m, n \in \mathbb{N}$. We denote vectors in bold and let $\mathbf{0} \in \mathbb{R}^n$ denote the 0-vector. Sets of polynomials are denoted by capital calligraphic letters. We denote the set of terms (or monomials) and the polynomial ring over \mathbb{R} in n variables by \mathcal{T} and \mathcal{P} , respectively. Given a polynomial $g \in \mathcal{P}$, let $\deg(g)$ denote its *degree*. The sets of polynomials in n variables of and up to degree $d \in \mathbb{N}$ are denoted by \mathcal{P}_d and $\mathcal{P}_{\leq d}$, respectively. Similarly, for a set of polynomials $\mathcal{G} \subseteq \mathcal{P}$, let $\mathcal{G}_d = \mathcal{G} \cap \mathcal{P}_d$ and $\mathcal{G}_{\leq d} = \mathcal{G} \cap \mathcal{P}_{\leq d}$. We often assume that $X = \{\mathbf{x}_1, \dots, \mathbf{x}_m\} \subseteq [0, 1]^n$, a form that can be realized, for example, via *min-max feature scaling*.⁶ Given a polynomial $g \in \mathcal{P}$ and a set of polynomials $\mathcal{G} = \{g_1, \dots, g_k\} \subseteq \mathcal{P}$, define the *evaluation vector* of g and *evaluation matrix* of \mathcal{G} over X as

$$g(X) = (g(\mathbf{x}_1), \dots, g(\mathbf{x}_m))^\top \in \mathbb{R}^m \quad \text{and} \quad \mathcal{G}(X) = (g_1(X), \dots, g_k(X)) \in \mathbb{R}^{m \times k},$$

respectively. Further, define the *mean squared error* of g over X as

$$\text{MSE}(g, X) = \frac{1}{m} \|g(X)\|_2^2.$$

2.2 Theoretical background

OAVI sequentially processes terms according to a so-called *term ordering*. For ease of presentation, we only consider the *degree-lexicographical ordering of terms* (DegLex) (Cox et al., 2013, Chapter 2), denoted by $<_\sigma$. Given, for example, the terms $t, u, v \in \mathcal{T}_1$, DegLex works as follows:

$$1 <_\sigma t <_\sigma u <_\sigma v <_\sigma t^2 <_\sigma tu <_\sigma tv <_\sigma u^2 <_\sigma uv <_\sigma v^2 <_\sigma t^3 <_\sigma \dots,$$

5. Monomial-aware algorithms are less susceptible to the spurious vanishing problem than monomial-agnostic algorithms.

6. With more complicated analysis, all our theoretical results can be generalized to $X \subseteq [-1, 1]^n$. For ease of presentation, we restrict ourselves to $X \subseteq [0, 1]^n$.

where 1 denotes the constant-1 term. Given a set of terms $\mathcal{O} = \{t_1, \dots, t_k\}_\sigma \subseteq \mathcal{T}$, the subscript σ indicates that $t_1 <_\sigma \dots <_\sigma t_k$, that is, that we consider the elements of \mathcal{O} in the order defined by σ . With the notion of term ordering, we can define the leading term (coefficient) of a polynomial.

Definition 2.1 (Leading term (coefficient)). Let $g = \sum_{i=1}^k c_i t_i \in \mathcal{P}$ and $j \in \{1, \dots, k\}$ such that $t_j >_\sigma t_i$ for all $i \in \{1, \dots, k\} \setminus \{j\}$. Then, t_j and c_j are called *leading term* and *leading term coefficient* of g , denoted by $\text{LT}(g) = t_j$ and $\text{LTC}(g) = c_j$, respectively.

We then define vanishing polynomials via the mean squared error.

Definition 2.2 (Approximately vanishing polynomial). Let $X = \{\mathbf{x}_1, \dots, \mathbf{x}_m\} \subseteq \mathbb{R}^n$ and $\psi \geq 0$. A polynomial $g \in \mathcal{P}$ is ψ -approximately vanishing (over X) if $\text{MSE}(g, X) \leq \psi$. Further, a ψ -approximately vanishing polynomial g over X with $\text{LTC}(g) = 1$ is called $(\psi, 1)$ -approximately vanishing (over X).

We fix the LTC of polynomials to prevent rescaling of polynomials, which addresses the spurious vanishing problem.

Definition 2.3 (Approximate vanishing ideal). Let $X = \{\mathbf{x}_1, \dots, \mathbf{x}_m\} \subseteq \mathbb{R}^n$ and $\psi \geq 0$. The ψ -approximate vanishing ideal (over X), \mathcal{I}_X^ψ , is the ideal generated by all $(\psi, 1)$ -approximately vanishing polynomials over X .

For $\psi = 0$, it holds that $\mathcal{I}_X^0 = \mathcal{I}_X$, that is, the approximate vanishing ideal becomes the vanishing ideal. Thus, Definition 2.3 subsumes the definition of the vanishing ideal. By Hilbert's basis theorem (Cox et al., 2013), for any ideal $\mathcal{I} \subseteq \mathcal{P}$, there exists a finite number of generators, $g_1, \dots, g_k \in \mathcal{I}$ with $k \in \mathbb{N}$, such that for any $h \in \mathcal{I}$, there exist $h_1, \dots, h_k \in \mathcal{P}$ such that

$$h = \sum_{i=1}^k g_i h_i.$$

Finally, we present the problem that OAVI addresses.

Problem 2.4 (Setting). Let $X = \{\mathbf{x}_1, \dots, \mathbf{x}_m\} \subseteq \mathbb{R}^n$ and $\psi \geq 0$. Construct a set of $(\psi, 1)$ -approximately vanishing generators of \mathcal{I}_X^ψ .

Recall that for terms $t, u \in \mathcal{T}$, t divides (or is a divisor of) u , denoted by $t \mid u$, if there exists $s \in \mathcal{T}$ such that $ts = u$, and if t does not divide u , we write $t \nmid u$. Finally, OAVI requires the definition below.

Definition 2.5 (Border). Let $\mathcal{O} \subseteq \mathcal{T}_{d-1}$. The (degree- d) border of \mathcal{O} is defined as

$$\partial_d \mathcal{O} = \{u \in \mathcal{T}_d : t \in \mathcal{O}_{\leq d-1} \text{ for all } t \in \mathcal{T}_{\leq d-1} \text{ such that } t \mid u\}.$$

3. The Oracle Approximate Vanishing Ideal algorithm (OAVI)

In this section, we recall the Oracle Approximate Vanishing Ideal algorithm (OAVI) (Wirth and Pokutta, 2022), a method for solving Problem 2.4. OAVI is presented in Algorithm 1.

3.1 Algorithm overview

For an in-depth explanation of OAVI, we refer to Sections 4 and 5 of Wirth and Pokutta (2022). Here, we only recall the main ideas: The algorithm takes as input a data set $X = \{\mathbf{x}_1, \dots, \mathbf{x}_m\} \subseteq [0, 1]^n$ and a vanishing parameter $\psi \geq 0$. Then, the algorithm constructs a finite set of $(\psi, 1)$ -approximately vanishing generators of the ψ -approximate vanishing ideal \mathcal{I}_X^ψ . Throughout, the algorithm keeps track of two sets: a set of terms $\mathcal{O} \subseteq \mathcal{T}$ such that there does not exist a generator of \mathcal{I}_X^ψ with terms only in \mathcal{O} and a set of generators $\mathcal{G} \subseteq \mathcal{P}$ of the ψ -approximate vanishing ideal \mathcal{I}_X^ψ . For every degree $d \geq 1$, the algorithm computes the set $\partial_d \mathcal{O}$ in Line 4, the degree- d border, see Definition 2.5. Then, in Lines 5–13, for every term $u \in \partial_d \mathcal{O}$, OAVI determines

Algorithm 1: OAVI

Input : $X = \{\mathbf{x}_1, \dots, \mathbf{x}_m\} \subseteq [0, 1]^n$ and $\psi \geq 0$.**Output** : $\mathcal{G} \subseteq \mathcal{P}$ and $\mathcal{O} \subseteq \mathcal{T}$.

```
1  $d \leftarrow 1$ 
2  $\mathcal{O} = \{t_1\}_\sigma \leftarrow \{1\}_\sigma$  ▷ The monomial 1 is the constant-1 monomial
3  $\mathcal{G} \leftarrow \emptyset$ 
4 while  $\partial_d \mathcal{O} = \{u_1, \dots, u_k\}_\sigma \neq \emptyset$  ▷ Repeat as long as the border is non-empty
5   for  $i = 1, \dots, k$  do
6      $\ell \leftarrow |\mathcal{O}| \in \mathbb{N}$ ,  $A \leftarrow \mathcal{O}(X) \in \mathbb{R}^{m \times \ell}$ ,  $\mathbf{b} \leftarrow u_i(X) \in \mathbb{R}^m$ 
7      $\mathbf{c} \in \operatorname{argmin}_{\mathbf{y} \in \mathbb{R}^\ell} \frac{1}{m} \|\mathbf{A}\mathbf{y} + \mathbf{b}\|_2^2$  ▷ Convex optimization oracle call
8      $g \leftarrow \sum_{j=1}^\ell c_j t_j + u_i$ 
9     if  $\operatorname{MSE}(g, X) \leq \psi$  then ▷ Check whether  $g$  vanishes  $(\psi, 1)$ -approximately
10       $\mathcal{G} \leftarrow \mathcal{G} \cup \{g\}$ 
11    else
12       $\mathcal{O} = \{t_1, \dots, t_{|\mathcal{O}|}\}_\sigma \leftarrow (\mathcal{O} \cup \{u_i\})_\sigma$ 
13    end
14  end
15   $d \leftarrow d + 1$ 
16 end
```

whether there exists a $(\psi, 1)$ -approximately vanishing generator g of \mathcal{I}_X^ψ with $\operatorname{LT}(g) = u$ and other terms only in \mathcal{O} via oracle access to a solver of the convex optimization problem in Line 7. If a $(\psi, 1)$ -approximately vanishing generator g exists, it gets appended to \mathcal{G} in Line 10. Otherwise, the term u gets appended to \mathcal{O} in Line 12. OAVI terminates when a degree $d \in \mathbb{N}$ is reached such that the $\partial_d \mathcal{O} = \emptyset$ (Wirth and Pokutta, 2022, Proposition 6.1). Then, \mathcal{G} is a set of generators of the ψ -approximate vanishing ideal of X and there does not exist a $(\psi, 1)$ -approximately vanishing polynomial with terms only in \mathcal{O} (Wirth and Pokutta, 2022, Theorem 6.2). Throughout, we denote the output of OAVI by \mathcal{G} and \mathcal{O} , that is, $(\mathcal{G}, \mathcal{O}) = \operatorname{OAVI}(X, \psi)$.

In practice, the optimization problem in Line 7 is only solved up to a certain tolerance, a subtlety we discuss in the remark below.

Remark 3.1 (On solver inaccuracy). In practice, the optimization problem in Line 7 of OAVI is addressed with solvers that determine an ε -accurate solution to the convex optimization problem, where $\varepsilon \geq 0$. The consequences of solving the optimization problem in Line 7 only to ε -accuracy are theoretically well-understood and have little impact on the performance of OAVI (Wirth and Pokutta, 2022, Theorem 6.2). For clarity, we thus restrict the majority of the analysis of OAVI to the case that solvers of the optimization problem in Line 7 are accurate.

3.2 Preprocessing with OAVI in a classification pipeline

In this section, we present an overview of how OAVI can be used as a feature transformation method for a subsequently applied linear kernel Support Vector Machine (SVM) with pseudocode presented in Algorithm 2. We follow the overview of Wirth and Pokutta (2022) and the notations of Mohri et al. (2018).

Setting. Let $X \subseteq [0, 1]^n$ and $\mathcal{Y} = \{1, \dots, k\}$ be an input and output space, respectively. We are given a training sample $S = \{(\mathbf{x}_1, y_1), \dots, (\mathbf{x}_m, y_m)\} \in (X \times \mathcal{Y})^m$ drawn *i.i.d.* from some unknown distribution \mathcal{D} . Our task is to determine a *hypothesis* $h: X \rightarrow \mathcal{Y}$ with small *generalization error*

$$\mathbb{P}_{(\mathbf{x}, y) \sim \mathcal{D}}[h(\mathbf{x}) \neq y].$$

Lines 1–5: generator construction. We apply OAVI as a preprocessing technique. Note that OAVI does not get applied to the entire data set $X = \{\mathbf{x}_1, \dots, \mathbf{x}_m\}$ at once but instead, once for each class. More specifically,

Algorithm 2: Preprocessing data with OAVI for a linear kernel SVM

Input : A training sample $S = \{(\mathbf{x}_1, y_1), \dots, (\mathbf{x}_m, y_m)\}$ with $X = \{\mathbf{x}_1, \dots, \mathbf{x}_m\} \subseteq [0, 1]^n$ and $y_1, \dots, y_m \in \{1, \dots, k\}$.

```
1 for  $i = 1, \dots, k$  do           ▶ Construct generators for the  $k$  classes, individually
2    $X^i \leftarrow \{\mathbf{x}_j \in X \mid y_j = i\} \subseteq X$            ▶ Samples corresponding to class  $i$ 
3    $(\mathcal{G}^i, \mathcal{O}^i) \leftarrow \text{OAVI}(X^i, \psi)$            ▶ Fit OAVI to samples corresponding to class  $i$ 
4 end
5  $\mathcal{G} = \{g_1, \dots, g_{|\mathcal{G}|}\} \leftarrow \bigcup_{i=1}^k \mathcal{G}^i$            ▶ Collect the generators of all classes
6 for  $j = 1, \dots, m$  do           ▶ Transform the training sample  $S \dots$ 
7    $\tilde{\mathbf{x}}_j \leftarrow (|g_1(\mathbf{x}_j)|, \dots, |g_{|\mathcal{G}|}(\mathbf{x}_j)|)^\top$  ▶ ...via the transformation induced by polynomials in  $\mathcal{G}$ 
8 end
9  $\tilde{S} \leftarrow \{(\tilde{\mathbf{x}}_1, y_1), \dots, (\tilde{\mathbf{x}}_m, y_m)\}$            ▶  $\tilde{S}$  is the feature-transformed data set
10 Train a linear kernel SVM on  $\tilde{S}$ 
```

for each class $i \in \{1, \dots, k\}$, let $X^i = \{\mathbf{x}_j \in X \mid y_j = i\} \subseteq X$ denote the subset of samples corresponding to class i . Then, for each class $i \in \{1, \dots, k\}$, we construct a set of $(\psi, 1)$ approximately vanishing generators \mathcal{G}^i of the ψ -approximate vanishing ideal $\mathcal{I}_{X^i}^\psi$ via a call to OAVI, that is, $(\mathcal{G}^i, \mathcal{O}^i) \leftarrow \text{OAVI}(X^i, \psi)$. Combining the sets of generators corresponding to the different classes, we obtain

$$\mathcal{G} = \{g_1, \dots, g_{|\mathcal{G}|}\} \leftarrow \bigcup_{i=1}^k \mathcal{G}^i,$$

which is a set of polynomials encapsulating the feature transformation we are about to apply to data set X .

Lines 6–9: applying the feature transformation. As proposed in Livni et al. (2013), we transform the training sample X via the feature transformation

$$\mathbf{x}_j \mapsto \tilde{\mathbf{x}}_j = (|g_1(\mathbf{x}_j)|, \dots, |g_{|\mathcal{G}|}(\mathbf{x}_j)|)^\top \in \mathbb{R}^{|\mathcal{G}|} \quad (\text{FT})$$

for $j = 1, \dots, m$. The motivation behind this feature transformation is that a polynomial $g \in \mathcal{G}^i$ vanishes approximately over all $\mathbf{x} \in X^i$ and (hopefully) attains values that are far from zero over points $\mathbf{x} \in X \setminus X^i$.

Line 10: training the support vector machine. We then train a linear kernel SVM on the feature-transformed data $\tilde{S} = \{(\tilde{\mathbf{x}}_1, y_1), \dots, (\tilde{\mathbf{x}}_m, y_m)\}$ with ℓ_1 -regularization to keep the number of used features as small as possible. As shown in Livni et al. (2013), if $\psi = 0$ and the underlying classes of S belong to disjoint algebraic sets, then the different classes become linearly separable in the feature space corresponding to transformation (FT) and a perfect classification accuracy is achieved with the linear kernel SVM.

3.3 On solver selection

In this section, we discuss the optimization problem in Line 7 of OAVI and the methods for solving it.

In Algorithm 1, we introduce OAVI with an unconstrained quadratic convex optimization problem in Line 7 of OAVI, which Wirth and Pokutta (2022) solved with *Accelerated Gradient Descent* (AGD) (Nesterov, 1983). Wirth and Pokutta (2022) also pointed out the advantages of considering the ℓ_1 -constrained version of the optimization problem in Line 7: In case the ℓ_1 -norm of the coefficient vectors of the generators in \mathcal{G} is bounded, the $(\psi, 1)$ -approximately vanishing generators in \mathcal{G} are guaranteed to also vanish on out-sample data and the combined approach of using generators obtained via OAVI to preprocess the data for a subsequently applied linear kernel SVM inherits the generalization bound of the SVM (Wirth and Pokutta, 2022, Theorems 6 and B.3, respectively). To guarantee that the coefficient vectors of constructed generators are bounded in the ℓ_1 -norm, it suffices to add ℓ_1 -ball constraints to the optimization problem in Line 7 of OAVI, resulting in the

following quadratic constrained convex optimization problem:

$$\mathbf{c} \leftarrow \operatorname{argmin}_{\mathbf{y} \in \mathbb{R}^\ell, \|\mathbf{y}\|_1 \leq \tau-1} \frac{1}{m} \|\mathbf{A}\mathbf{y} + \mathbf{b}\|_2^2, \quad (\text{CCOP})$$

where $\tau - 1 \geq 1$ is the radius of the ℓ_1 -ball. If the optimization problem in Line 7 of OAVI is replaced with (CCOP), then OAVI constructs generators that are $(\psi, 1)$ -approximately vanishing and whose coefficient vectors are τ -bounded in the ℓ_1 -norm. Since (CCOP) is not unconstrained, we solve (CCOP) with variants of the Frank-Wolfe algorithm, a.k.a. Conditional Gradients algorithm (CG) to create coefficient vectors that are sparse, a widely exploited property of Frank-Wolfe algorithms (Pokutta et al., 2020; Carderera et al., 2021).

In summary, by replacing the optimization problem in Line 7 of OAVI with (CCOP), OAVI satisfies several generalization bounds and by solving (CCOP) with CG variants, the constructed generators become sparse.

4. OAVI at scale

Despite the strong theoretical results proved in Wirth and Pokutta (2022), OAVI and related algorithms such as ABM and VCA all admit time, space, and evaluation⁷ complexities that depend superlinearly on m , where m is the number of samples in the data set $X = \{\mathbf{x}_1, \dots, \mathbf{x}_m\} \subseteq [0, 1]^n$ (Limbeck, 2013; Livni et al., 2013; Wirth and Pokutta, 2022). Thus, up until now, algorithms constructing generators for the approximate vanishing ideal were often overlooked by practitioners that work at scale. In this section, we address this issue with a tighter analysis of the computational complexities of OAVI and related monomial-aware algorithms and with modifications to OAVI that reduce the training time by up to multiple orders of magnitude. We first recall OAVI’s computational complexity and then detail the different approaches to improve the computational complexity of OAVI.

4.1 OAVI’s computational complexity

The analysis of the computational complexity for OAVI hinges on two factors: finding a tight bound on the number of times the convex optimization oracle gets called to solve the optimization problem in Line 7 of OAVI (or the constrained problem (CCOP)) and the cost of a solver call. During OAVI’s execution, the convex solver gets called exactly once per term in any of the borders, for a total of $|\mathcal{G}| + |\mathcal{O}| - 1$ calls, where $(\mathcal{G}, \mathcal{O}) = \text{OAVI}(X, \psi)$ for a data set $X = \{\mathbf{x}_1, \dots, \mathbf{x}_m\} \subseteq [0, 1]^n$ and vanishing parameter $\psi \geq 0$. Below, we recall the computational complexity of OAVI expressed in dependence of $|\mathcal{G}| + |\mathcal{O}|$.

Theorem 4.1 (Time and space complexity (Wirth and Pokutta, 2022, Theorem 6.4)). *Let $X = \{\mathbf{x}_1, \dots, \mathbf{x}_m\} \subseteq [0, 1]^n$, $\psi \geq 0$, and $(\mathcal{G}, \mathcal{O}) = \text{OAVI}(X, \psi)$. In the real number model, the time and space complexities of OAVI are $O((|\mathcal{G}| + |\mathcal{O}|)^2 + (|\mathcal{G}| + |\mathcal{O}|)T_{\text{ORACLE}})$ and $O((|\mathcal{G}| + |\mathcal{O}|)m + S_{\text{ORACLE}})$, where T_{ORACLE} and S_{ORACLE} are the time and space complexities required to solve the convex optimization problem in Line 7 of OAVI (or (CCOP)), respectively.*

Theorem 4.2 (Evaluation complexity (Wirth and Pokutta, 2022, Theorem 6.5)). *Let $X = \{\mathbf{x}_1, \dots, \mathbf{x}_m\} \subseteq [0, 1]^n$, $\psi \geq 0$, and $(\mathcal{G}, \mathcal{O}) = \text{OAVI}(X, \psi)$. In the real number model, we can compute the evaluation vectors of all polynomials in \mathcal{G} over a set $Z = \{\mathbf{z}_1, \dots, \mathbf{z}_q\} \subseteq [0, 1]^n$ in time $O((|\mathcal{G}| + |\mathcal{O}|)^2 q)$.*

Under mild assumptions, Wirth and Pokutta (2022) proved that $O(|\mathcal{G}| + |\mathcal{O}|) = O(mn)$, implying that OAVI’s computational complexity is superlinear in m . We pursue two avenues to improve the computational complexity and time complexity, in particular, of OAVI:

1. **Reduction of the magnitude of $|\mathcal{G}| + |\mathcal{O}|$:** In Section 4.2, we derive a number-of-samples-agnostic bound on $|\mathcal{G}| + |\mathcal{O}|$. Then, the time and space complexities of OAVI are linear in m and polynomial in n and the evaluation complexity of OAVI is independent of m and polynomial in n .
2. **Faster solving of the optimization problem in Line 7 of OAVI (or (CCOP)):** In Section 4.3, for the ℓ_1 -constrained optimization problem (CCOP), we replace the Pairwise Conditional Gradients

⁷ In this context, the evaluation complexity is the time required to evaluate all generators in \mathcal{G} on previously unseen data.

algorithm (PCG) used in [Wirth and Pokutta \(2022\)](#) with the faster Blended Pairwise Conditional Gradients algorithm (BPCG), exponentially improving the dependence of the time complexity of OAVI on $|\mathcal{G}| + |\mathcal{O}|$. Finally, in Section 4.4, we explain how to efficiently incorporate information on the inverse of the Hessian of the optimization problem in Line 7 of OAVI (or (CCOP)) to massively improve the time complexity of T_{ORACLE} and, thus, the time complexity of OAVI , with Inverse Hessian Boosting (IHB).

4.2 Number-of-samples-agnostic bound on $|\mathcal{G}| + |\mathcal{O}|$

For $X = \{\mathbf{x}_1, \dots, \mathbf{x}_m\} \subseteq [0, 1]^n$, $\psi \geq 0$, and $(\mathcal{G}, \mathcal{O}) = \text{OAVI}(X, \psi)$, the bound $|\mathcal{G}| + |\mathcal{O}| = O(mn)$ ([Wirth and Pokutta, 2022](#)) implies that the number of constructed generators depends on the number of samples in X and is independent of the vanishing parameter ψ . However, in the practical setting where ψ is sufficiently larger than 0 to avoid overfitting to noisy data and m is large, a dependence of $|\mathcal{G}| + |\mathcal{O}|$ on m is not intuitive. Indeed, a polynomial $g \in \mathcal{P}$ is ψ -approximately vanishing if $\text{MSE}(g, X) = \frac{1}{m} \|g(X)\|_2^2 \leq \psi$, that is, when, on average, $(g(\mathbf{x}))^2$ is smaller than ψ for $\mathbf{x} \in X$. Thus, there is a priori no reason that the number of samples m should determine the number of generators constructed by OAVI . Below, in contrast to most of the literature ([Heldt et al., 2009](#); [Fassino, 2010](#); [Limbeck, 2013](#); [Livni et al., 2013](#); [Wirth and Pokutta, 2022](#)), where the analysis of generator-constructing algorithms assumes that $\psi = 0$, we exploit $\psi > 0$ to prove the number-of-samples-agnostic bound $|\mathcal{G}| + |\mathcal{O}| = O((- \log(\psi) + n)^{-\log \psi})$.

Theorem 4.3 (Number-of-samples-agnostic bound on $|\mathcal{G}| + |\mathcal{O}|$). *Let $X = \{\mathbf{x}_1, \dots, \mathbf{x}_m\} \subseteq [0, 1]^n$, $\psi \in]0, 1[$, and $(\mathcal{G}, \mathcal{O}) = \text{OAVI}(X, \psi)$. Then, $|\mathcal{G}| + |\mathcal{O}| \leq \binom{D+n}{D}$, where $D = \lceil -\log(\psi)/\log(4) \rceil$ is the degree at which OAVI terminates.*

Proof. Let $X = \{\mathbf{x}_1, \dots, \mathbf{x}_m\} \subseteq [0, 1]^n$ and let $t_1, \dots, t_n \in \mathcal{T}_1$ be the degree-1 monomials. Suppose that during OAVI 's execution, for some degree $d \in \mathbb{N}$, OAVI checks whether the term $u = \prod_{j=1}^n t_j^{\alpha_j} \in \partial_d \mathcal{O}$, where $\sum_{j=1}^n \alpha_j = d$ and $\alpha_j \in \mathbb{N}$ for all $j \in \{1, \dots, n\}$, is the leading term of a $(\psi, 1)$ -approximately vanishing generator with non-leading terms only in \mathcal{O} . Let

$$h = \prod_{j=1}^n \left(t_j - \frac{1}{2} \mathbb{1} \right)^{\alpha_j}, \quad (4.1)$$

where $\mathbb{1}$ denotes the constant-1 monomial, that is, $\mathbb{1}(\mathbf{x}) = 1$ for any $\mathbf{x} \in \mathbb{R}^n$. Since $u \in \partial_d \mathcal{O}$, for any term $t \in \mathcal{T}$ such that $t \mid u$ and $t \neq u$, it holds that $t \in \mathcal{O}$ and, thus, h is a polynomial with $\text{LTC}(h) = 1$, $\text{LT}(h) = u$, and other terms only in \mathcal{O} . Under the assumption that the convex optimization oracle in OAVI is accurate, $\text{MSE}(h, X) \geq \text{MSE}(g, X)$, where g is the polynomial constructed during Lines 7 and 8 of OAVI . Hence, proving that h vanishes approximately implies that g vanishes approximately. Recalling that $t(\mathbf{x}) \in [0, 1]$ for all $\mathbf{x} \in X$ and $t \in \mathcal{T}_1$, it holds that $|t(\mathbf{x}) - \frac{1}{2}| \leq \frac{1}{2}$ for all $\mathbf{x} \in X$ and $t \in \mathcal{T}_1$. Thus,

$$\text{MSE}(g, X) \leq \text{MSE}(h, X) = \frac{1}{m} \|h\|_2^2 = \frac{1}{m} \sum_{\mathbf{x} \in X} \left(\prod_{j=1}^n \left(t_j(\mathbf{x}) - \frac{1}{2} \mathbb{1}(\mathbf{x}) \right)^{\alpha_j} \right)^2 \leq \max_{\mathbf{x} \in X} \prod_{j=1}^n \left| t_j(\mathbf{x}) - \frac{1}{2} \right|^{2\alpha_j} \leq 4^{-d}.$$

Since $\text{MSE}(g, X) \leq 4^{-d} \leq \psi$ is satisfied for $d \geq D := \left\lceil -\frac{\log(\psi)}{\log(4)} \right\rceil$, OAVI terminates after reaching degree D . Thus, at the end of OAVI 's execution, $|\mathcal{G}| + |\mathcal{O}| \leq \binom{D+n}{D} \leq (D+n)^D$. \square

The number-of-samples-agnostic bound on $|\mathcal{G}| + |\mathcal{O}|$ derived in Theorem 4.3 implies that the time and space complexities of OAVI are linear in m and the evaluation complexity of OAVI does not depend on m . We illustrate in Figure 1 and discuss in the remark below.

Remark 4.4 (Computational complexities of OAVI and ABM). Under the assumption that T_{ORACLE} and S_{ORACLE} are linear in m and polynomial in $|\mathcal{G}| + |\mathcal{O}|$, Theorem 4.3 combined with Theorems 4.1 and 4.2 shows that the time and space complexities of OAVI are linear in m and polynomial in n and the evaluation complexity of OAVI does not depend on m and is polynomial in n . The magnitude of $|\mathcal{G}| + |\mathcal{O}|$ is not only a bottleneck for OAVI 's computational complexity but also for ABM. Since ABM can construct the polynomial $h/\|h\|_2$, where h is as in (4.1), ABM admits the same bound on $|\mathcal{G}| + |\mathcal{O}|$ as OAVI and a similar computational complexity as OAVI .

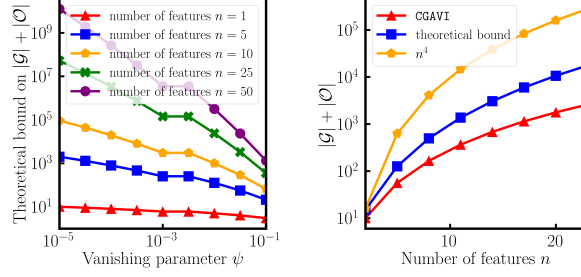


Figure 1: Left: Log-log plot of the bound on $|\mathcal{G}| + |\mathcal{O}|$ due to Theorem 4.3 versus the chosen vanishing parameter ψ for various numbers of features $n \in \mathbb{N}$ of the data set. The plot illustrates the polynomial and exponential dependencies of $|\mathcal{G}| + |\mathcal{O}|$ on n and ψ , respectively.

Right: A log-linear comparison of the theoretical bound on $|\mathcal{G}| + |\mathcal{O}|$ due to Theorem 4.3 and empirical $|\mathcal{G}| + |\mathcal{O}|$, where $(\mathcal{G}, \mathcal{O}) = \text{CGAVI}(X, \psi)$ for $\psi = 0.005$, CGAVI indicates that OAVI is run with CG, and $X \subseteq [0, 1]^n$ is a random data set of 10,000 samples and a varying number of features $n \in \mathbb{N}$. We also plot n^4 for better understanding of the results. The results are averaged over 10 runs and standard deviations are shaded but 0 throughout. In practice, $|\mathcal{G}| + |\mathcal{O}|$ is slightly smaller than predicted by Theorem 4.3.

In case we replace the optimization problem in Line 7 of OAVI with (CCOP), we have to choose $\tau \geq 2$ large enough to guarantee that $h \in \mathcal{P}$ as in (4.1) can be constructed. We discuss in the remark below.

Remark 4.5 (Termination for OAVI with (CCOP)). In case OAVI is run with (CCOP) instead of the optimization problem in Line 7, $\tau \geq 2$ has to be chosen large enough to guarantee that the ℓ_1 -norm of the coefficient vector of h as in (4.1) is smaller than τ for Theorem 4.3 to apply. By induction, for h as in (4.1) of degree d , it holds that $\|h\|_1 \leq (\frac{3}{2})^d$. Thus, setting $\tau \geq (\frac{3}{2})^D$, where $D = \lceil -\log(\psi)/\log(4) \rceil$ guarantees that OAVI enjoys the bound on $|\mathcal{G}| + |\mathcal{O}|$ due to Theorem 4.3.

Note that the assumption $X \subseteq [0, 1]^n$ in Theorem 4.3 can be relaxed. In the proof of Theorem 4.3, we only require that $\|x\|_\infty \leq 1$ for all $x \in X$. Thus, all our theoretical results can be generalized to $X \subseteq [-1, 1]^n$ with appropriately adjusted constants.

4.3 The Blended Pairwise Conditional Gradients algorithm (BPCG)

We illustrate that improvements in performance of solvers of the optimization problem in Line 7 of OAVI and (CCOP) improve the training time of OAVI. Wirth and Pokutta (2022) used Accelerated Gradient Descent (AGD) and the Pairwise Conditional Gradients algorithm (PCG) to solve the optimization problem in Line 7 of OAVI and (CCOP), respectively. Whenever a faster solver for aforementioned convex optimization problems is introduced, the training time of OAVI is reduced as well. By replacing PCG with the Blended Pairwise Conditional Gradients algorithm (BPCG), presented in Algorithm 3, we drastically improve the time complexity of OAVI: The time complexity of BPCGAVI (OAVI with BPCG) is polynomial in $|\mathcal{G}| + |\mathcal{O}|$ as opposed to PCGAVI's (OAVI with PCG) time complexity, which is exponential in $|\mathcal{G}| + |\mathcal{O}|$.

Both PCG and BPCG are used to address constrained convex optimization problems of the form

$$y^* \in \operatorname{argmin}_{y \in P} f(y), \quad (4.2)$$

where $P \subseteq \mathbb{R}^\ell$ for $\ell \in \mathbb{N}$ is a polytope and $f: \mathbb{R}^\ell \rightarrow \mathbb{R}$ is a $(\mu$ -strongly) convex and L -smooth function. (4.2) subsumes (CCOP), that is, (CCOP) is a special case of (4.2). With $\operatorname{vert}(P)$ denoting the set of vertices of P , recall the convergence rate of PCG for solving (4.2).

Theorem 4.6 (Convergence rate of PCG (Lacoste-Julien and Jaggi, 2015)). *Let $P \subseteq \mathbb{R}^\ell$ be a polytope with pyramidal width ω and diameter δ and let f be a μ -strongly convex and L -smooth function. Then, for the*

Algorithm 3: BPCG

Input : A smooth and convex function f , a starting vertex $\mathbf{y}_0 \in \text{vert}(P)$.

Output : A point $\mathbf{y}_T \in P$.

```
1  $S^{(0)} \leftarrow \{\mathbf{y}_0\}$ 
2  $\lambda_{\mathbf{v}}^{(0)} \leftarrow 1$  for  $\mathbf{v} = \mathbf{y}_0$  and 0 otherwise
3 for  $t = 0, \dots, T$  do
4    $\mathbf{a}_t \in \arg\max_{\mathbf{v} \in S^{(t)}} \langle \nabla f(\mathbf{y}_t), \mathbf{v} \rangle$  ▷ Away vertex
5    $\mathbf{s}_t \in \arg\min_{\mathbf{v} \in S^{(t)}} \langle \nabla f(\mathbf{y}_t), \mathbf{v} \rangle$  ▷ Local FW vertex
6    $\mathbf{w}_t \in \arg\min_{\mathbf{v} \in \text{vert}(P)} \langle \nabla f(\mathbf{y}_t), \mathbf{v} \rangle$  ▷ FW vertex
7   if  $\langle \nabla f(\mathbf{y}_t), \mathbf{w}_t - \mathbf{y}_t \rangle \geq \langle \nabla f(\mathbf{y}_t), \mathbf{s}_t - \mathbf{a}_t \rangle$  then
8      $\mathbf{d}_t \leftarrow \mathbf{s}_t - \mathbf{a}_t$ 
9      $\gamma_t \in \arg\min_{\gamma \in [0, \lambda_{\mathbf{a}_t}^{(t)}]} f(\mathbf{y}_t + \gamma \mathbf{d}_t)$ 
10     $\lambda_{\mathbf{s}_t}^{(t+1)} \leftarrow \lambda_{\mathbf{s}_t}^{(t)} + \gamma_t$ 
11     $\lambda_{\mathbf{a}_t}^{(t+1)} \leftarrow \lambda_{\mathbf{a}_t}^{(t)} - \gamma_t$ 
12  else
13     $\mathbf{d}_t \leftarrow \mathbf{w}_t - \mathbf{y}_t$ 
14     $\gamma_t \in \arg\min_{\gamma \in [0, 1]} f(\mathbf{y}_t + \gamma \mathbf{d}_t)$ 
15     $\lambda_{\mathbf{v}}^{(t+1)} \leftarrow (1 - \gamma_t) \lambda_{\mathbf{v}}^{(t)}$  for  $\mathbf{v} \in S^{(t)}$ 
16     $\lambda_{\mathbf{w}_t}^{(t+1)} \leftarrow \begin{cases} \gamma_t, & \mathbf{w}_t \notin S^{(t)} \\ \lambda_{\mathbf{w}_t}^{(t)} + \gamma_t, & \mathbf{w}_t \in S^{(t)} \end{cases}$ 
17  end
18   $S^{(t+1)} \leftarrow \{\mathbf{v} \in \text{vert}(P) \mid \lambda_{\mathbf{v}}^{(t+1)} > 0\}$ 
19   $\mathbf{y}_{t+1} \leftarrow \mathbf{y}_t + \gamma_t \mathbf{d}_t$ 
20 end
```

sequence of iterates $\{\mathbf{y}_t\}_{t=0}^T \subseteq P$ of PCG, it holds that

$$f(\mathbf{y}_T) - f(\mathbf{y}^*) \leq (f(\mathbf{y}_0) - f(\mathbf{y}^*))e^{-\rho_{\text{PCG}}T},$$

where $\mathbf{y}_0 \in P$ is the starting point, \mathbf{y}^* is the optimal solution to (4.2), and $\rho_{\text{PCG}} = \frac{\mu\omega^2}{4L\delta^2(3|\text{vert}(P)|+1)}$.

The main improvement of BPCG over PCG is the removal of so-called *swap-steps*, that is, steps which shift weight from the away to the Frank-Wolfe vertex but do not lead to a lot of progress, see Tsuji et al. (2021). The large number of swap-steps in PCG leads to a dependence of the convergence rate on $(3|\text{vert}(P)|+1)$. Thus, to reach an ε -accurate solution, PCG requires a number of iterations that is exponential in the problem dimension. For (CCOP), the problem dimension is $|\mathcal{O}|$, which can be of similar order of magnitude to $|\mathcal{G}|+|\mathcal{O}|$. Thus, PCG can require a number of iterations that is exponential in $|\mathcal{G}|+|\mathcal{O}|$. In contrast, the convergence rate of BPCG does not depend on $(3|\text{vert}(P)|+1)$ and is, thus, polynomial in $|\mathcal{G}|+|\mathcal{O}|$. We recall BPCG's convergence rate for solving (4.2).

Theorem 4.7 (Convergence rate of BPCG (Tsuji et al., 2021)). *Let $P \subseteq \mathbb{R}^\ell$ be a polytope with pyramidal width ω and diameter δ and let f be a μ -strongly convex and L -smooth function. Then, for the sequence of iterates $\{\mathbf{y}_t\}_{t=0}^T \subseteq P$ of BPCG, it holds that*

$$f(\mathbf{y}_T) - f(\mathbf{y}^*) \leq (f(\mathbf{y}_0) - f(\mathbf{y}^*))e^{-\rho_{\text{BPCG}}T},$$

where $\mathbf{y}_0 \in P$ is the starting point, \mathbf{y}^* is the optimal solution to (4.2), and $\rho_{\text{BPCG}} = \frac{1}{2} \min \left\{ \frac{1}{2}, \frac{\mu\omega^2}{4L\delta^2} \right\}$.

Since the pyramidal width of the ℓ_1 -ball of radius $\tau - 1$ is at least $(\tau - 1)/\sqrt{\ell}$, see Lemma B.1, BPCG requires at most $T = \left\lceil \frac{32L\ell}{\mu} \log \left(\frac{f(\mathbf{y}_0) - f(\mathbf{y}^*)}{\varepsilon} \right) \right\rceil$ iterations to construct an ε -accurate solution to (CCOP), where

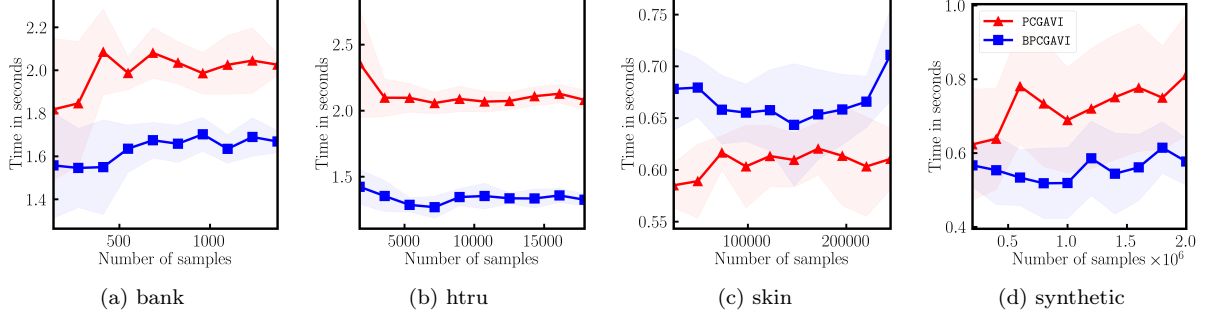


Figure 2: Comparison of the training times of PCGAVI and BPCGAVI with fixed $\psi = 0.005$ for a varying number of training samples for the bank, htru, skin, and synthetic data sets. The results are averaged over 10 runs and standard deviations are shaded. On all data sets except skin, BPCGAVI is faster than PCGAVI.

$A = O(X) \in \mathbb{R}^{m \times \ell}$ and μ and L are the smallest and largest eigenvalues of matrix $A^\top A \in \mathbb{R}^{\ell \times \ell}$, respectively. In BPCG, we first compute $A^\top A$ and $A^\top \mathbf{b}$, which, as explained in the proof of Theorem 4.9, requires $O(m\ell)$ elementary operations during OAVI’s execution via efficient updates, and then, BPCG’s per iteration cost is $O(\ell^2)$. Thus, ignoring dependencies on μ , L , and ε , it holds that $T_{\text{BPCG}} = O((|\mathcal{G}| + |\mathcal{O}|)m + (|\mathcal{G}| + |\mathcal{O}|)^3)$, which is an exponential improvement in $|\mathcal{G}| + |\mathcal{O}|$ compared to PCG. We summarize below, referring to OAVI with solver BPCG as BPCGAVI.

Corollary 4.8 (Computational complexity of BPCGAVI). *Let $X = \{\mathbf{x}_1, \dots, \mathbf{x}_m\} \subseteq [0, 1]^n$, $\psi > 0$, and $(\mathcal{G}, \mathcal{O}) = \text{BPCGAVI}(X, \psi)$. In the real number model, the time and space complexities of BPCGAVI are $O((|\mathcal{G}| + |\mathcal{O}|)^2 m + (|\mathcal{G}| + |\mathcal{O}|)^4)$ and $O((|\mathcal{G}| + |\mathcal{O}|)m + (|\mathcal{G}| + |\mathcal{O}|)^2)$, respectively.*

The numerical results in Figure 2 show that replacing PCG with BPCG in OAVI often leads to empirical speed-ups of OAVI. Thus, we suggest using BPCG as the default solver to address problem (CCOP) in OAVI. For the skin data set, BPCG’s tendency to construct sparser solutions than PCG is a possible explanation why BPCGAVI is slower than PCGAVI, but the phenomenon is not fully understood.

4.4 Inverse Hessian Boosting (IHB)

In this section, we introduce Inverse Hessian Boosting (IHB), a technique that speeds up the running time of OAVI by multiple orders of magnitudes by exploiting the structure of the optimization problems solved in OAVI. IHB provides a starting point to AGD or BPCG that is close to the optimal solution of the optimization problem in Line 7 of OAVI or (CCOP), respectively, to massively reduce the cost of oracle calls in OAVI.

4.4.1 MOTIVATION

We motivate IHB for the optimization problem in Line 7 of OAVI, which we address with AGD, and then discuss changes to IHB for OAVI with (CCOP) and BPCG in Section 4.4.3. Letting $\ell = |\mathcal{O}|$, $A = O(X) \in \mathbb{R}^{m \times \ell}$, $\mathbf{b} = u_i(X) \in \mathbb{R}^m$, and $f(\mathbf{y}) = \frac{1}{m} \|\mathbf{A}\mathbf{y} + \mathbf{b}\|_2^2$, the optimization problem in Line 7 of OAVI takes the form

$$\mathbf{c} \in \operatorname{argmin}_{\mathbf{y} \in \mathbb{R}^\ell} f(\mathbf{y}).$$

Then, the gradient and Hessian of f at $\mathbf{y} \in \mathbb{R}^\ell$ are

$$\nabla f(\mathbf{y}) = \frac{2}{m} A^\top (\mathbf{A}\mathbf{y} + \mathbf{b}) \in \mathbb{R}^\ell \quad \text{and} \quad \nabla^2 f(\mathbf{y}) = \frac{2}{m} A^\top A \in \mathbb{R}^{\ell \times \ell},$$

respectively. By construction, the columns of $A = O(X)$ are linearly independent. Hence, $A^\top A$ is positive definite and invertible, f is strongly convex, the solution \mathbf{c} to the optimization problem in Line 7 of OAVI is unique, and for $\mathbf{y} \in \mathbb{R}^\ell$, $\nabla f(\mathbf{y}) = \mathbf{0}$, if and only if $\mathbf{y} = \mathbf{c}$. Thus, the optimal solution to the optimization problem in Line 7 of OAVI is given by

Algorithm 4: IHB for AGD

Input : An optimization problem $\operatorname{argmin}_{\mathbf{y} \in \mathbb{R}^\ell} \frac{1}{m} \|\mathbf{A}\mathbf{y} + \mathbf{b}\|_2^2$, where $A \in \mathbb{R}^{m \times \ell}$ and $\mathbf{b} \in \mathbb{R}^m$, and $\varepsilon > 0$.

Output : An ε -accurate solution \mathbf{c} to the optimization problem.

- 1 $\mathbf{y}_0 \leftarrow (A^\top A)^{-1} A^\top \mathbf{b} \in \mathbb{R}^\ell$
 - 2 Solve $\mathbf{c} \in \operatorname{argmin}_{\mathbf{y} \in \mathbb{R}^\ell} \frac{1}{m} \|\mathbf{A}\mathbf{y} + \mathbf{b}\|_2^2$ to ε -accuracy with AGD using \mathbf{y}_0 as a starting vector
-

$\mathbf{c} = (A^\top A)^{-1} A^\top \mathbf{b} \in \mathbb{R}^\ell$. In theory, it is thus no longer necessary to call a convex solver to solve the optimization problem in Line 7 of OAVI, which can lead to massive speed-ups in OAVI. Since matrix inversions are numerically unstable and relying on them would make OAVI less robust, we instead capitalize on the fact that, for AGD, the number of iterations to reach an ε -accurate solution to the optimization problem in Line 7 of OAVI depends on the Euclidean distance between the starting vector and the optimal solution.

4.4.2 ALGORITHM OVERVIEW

Inverse Hessian Boosting (IHB) is presented for AGDAVI (OAVI with AGD) in Algorithm 4: In AGDAVI, instead of running AGD to solve the optimization problem in Line 7 of OAVI directly, we first compute $\mathbf{y}_0 \leftarrow (A^\top A)^{-1} A^\top \mathbf{b} \in \mathbb{R}^\ell$ and use \mathbf{y}_0 as a starting vector for AGD. Since \mathbf{y}_0 is a well-educated guess for the optimal solution of the optimization problem in Line 7 of OAVI, \mathbf{y}_0 is often an ε -accurate solution to the optimization problem and AGD does not need to be run for more than 1 iteration. In case $(A^\top A)^{-1}$ is not computed correctly, AGD still guarantees an ε -accurate solution to the optimization problem. In Section 4.4.3, we extend IHB to OAVI with (CCOP).

4.4.3 IHB WITH ℓ_1 -CONSTRAINTS

Feasibility. IHB requires that the columns of A are linearly independent such that $A^\top A$ is invertible, which is guaranteed for AGDAVI but not for OAVI with (CCOP): Suppose that OAVI currently executes Lines 7–12 with the unconstrained optimization problem in Line 7 replaced by (CCOP) for a particular term $u_i \in \partial_d \mathcal{O}$. With $\ell = |\mathcal{O}|$, $A = \mathcal{O}(X) \in \mathbb{R}^{m \times \ell}$, $\mathbf{b} = u_i(X) \in \mathbb{R}^m$, and $f(\mathbf{y}) = \frac{1}{m} \|\mathbf{A}\mathbf{y} + \mathbf{b}\|_2^2$, (CCOP) becomes

$$\mathbf{c} \in \operatorname{argmin}_{\mathbf{y} \in \mathbb{R}^\ell, \|\mathbf{y}\|_1 \leq \tau-1} f(\mathbf{y}).$$

Let $\mathbf{y}_0 = (A^\top A)^{-1} A^\top \mathbf{b}$, but suppose that \mathbf{y}_0 is not a feasible starting vector for (CCOP), that is,

$$\|\mathbf{y}_0\|_1 = \|(A^\top A)^{-1} A^\top \mathbf{b}\|_1 > \tau - 1, \quad (\text{INF})$$

that polynomial $g = \sum_{j=1}^\ell c_j t_j + u_i$ constructed in Line 8 of OAVI does not vanish approximately, and that there exists $h \in \mathcal{P}$ with $\text{LT}(h) = u_i$, $\text{LTC}(h) = 1$, non-leading terms only in \mathcal{O} , and coefficient vector ℓ_1 -norm greater than τ that vanishes exactly over X , that is, $\text{MSE}(h, X) = 0 \leq \psi < \text{MSE}(g, X)$. Then, OAVI updates $\mathcal{O} \leftarrow (\mathcal{O} \cup \{u_i\})_\sigma$ and $A \leftarrow (A, \mathbf{b}) \in \mathbb{R}^{m \times (\ell+1)}$. Since $\text{MSE}(h, X) = 0$, the columns of the updated A are linearly dependent, $(A^\top A)^{-1}$ is not defined, and IHB is no longer applicable. We present two approaches to address this issue for OAVI with (CCOP):

- Instead of choosing a fixed $\tau \geq 2$ for all solver calls, determine τ for each solver call individually such that (INF) never occurs, that is, always choose τ such that $\tau \geq 1 + \|\mathbf{y}_0\|_1 = 1 + \|(A^\top A)^{-1} A^\top \mathbf{b}\|_1$. This approach jeopardizes the generalization properties of OAVI, which rely on τ being a constant.
- An alternative is to use a fixed $\tau \geq 2$ and to stop using IHB as soon as the assumptions of Theorem 4.9 could be violated, that is, when (INF) holds. This approach preserves the generalization bounds of OAVI and is implemented in our codebase with $\tau = 1000$.

Sparsity and Weak Inverse Hessian Boosting (WIHB). The benefit of using CG variants to solve (CCOP) is that the solution vector tends to be sparse. However, by initializing CG with $\mathbf{y}_0 = (A^\top A)^{-1} A^\top \mathbf{b}$, CG starts with a non-sparse iterate, which leads to a non-sparse coefficient vector of the polynomial constructed in Line 8 of CGDAVI (OAVI with solver CG). In case we use PCG or BPCG to solve (CCOP), we also need to represent the initial vector \mathbf{y}_0 as a convex combination of vertices. Thus, in practice, when we are not interested in

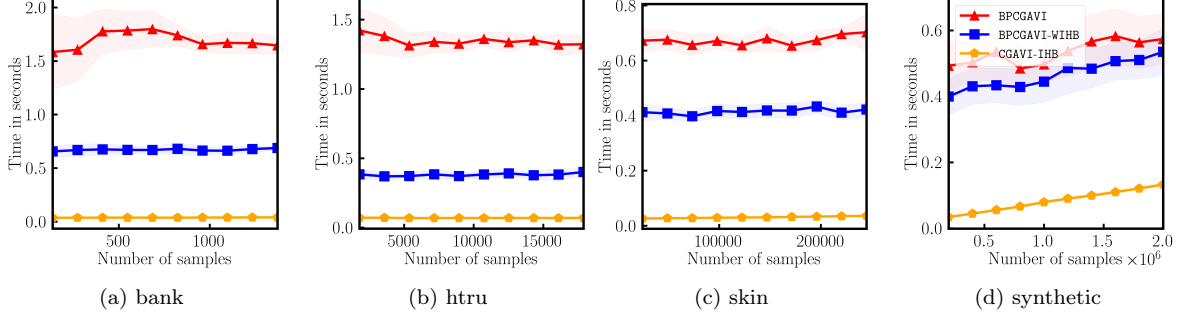


Figure 3: Comparison of the training times of BPCGAVI, BPCGAVI-WIHB, and CGAVI-IHB with fixed $\psi = 0.005$ for a varying number of training samples for the bank, htru, skin, and synthetic data sets. The results are averaged over 10 runs and standard deviations are shaded. For synthetic, the linear dependence of the training time on the number of training samples is apparent. On all data sets, CGAVI-IHB is faster than BPCGAVI-WIHB, which is faster than BPCGAVI.

sparse generators, we only use IHB with CGAVI, referring to the resulting algorithm as CGAVI-IHB. In case we require sparse generators, we propose *Weak Inverse Hessian Boosting* (WIHB) with BPCGAVI, referred to as BPCGAVI-WIHB: In OAVI, we first use IHB to quickly solve (CCOP) with CG to determine whether a specific term is the leading term of a $(\psi, 1)$ -approximately vanishing generator. If the corresponding polynomial constructed in Line 8 of OAVI vanishes approximately, then we solve (CCOP) again with BPCG and a vertex of the feasible region as initial vector to obtain a generator in Line 8 of OAVI whose coefficient vector is sparse. If the corresponding polynomial does not vanish approximately, then we do not have to solve (CCOP) again. Thus, BPCGAVI-WIHB solves (CCOP) with BPCG $|\mathcal{G}|$ times as opposed to, for example, BPCGAVI, which solves (CCOP) with BPCG $|\mathcal{G}| + |\mathcal{O}| - 1$ times. Thus, BPCGAVI-WIHB combines the sparsity-inducing properties of BPCG with the speed-up of IHB.

4.4.4 COMPUTATIONAL COMPLEXITY

The main cost of IHB is the inversion of the matrix $A^\top A \in \mathbb{R}^{\ell \times \ell}$, which generally requires $O(\ell^3)$ elementary operations. Since OAVI solves a series of quadratic convex optimization problems that differ from each other only slightly, we can maintain and update $(A^\top A)^{-1}$ using $O(\ell^2)$ instead of $O(\ell^3)$ elementary operations.

When OAVI is run with (CCOP), we assume that $\tau \geq 2$ is large enough to guarantee that (INF) never holds, that is, $A^\top A$ is invertible. Consider OAVI's execution of Lines 7–12 for a particular term $u_i \in \partial_d \mathcal{O}$. Let $\ell = |\mathcal{O}|$, $A = \mathcal{O}(X) \in \mathbb{R}^{m \times \ell}$, $\mathbf{b} = u_i(X)$, and $f(\mathbf{y}) = \frac{1}{m} \|\mathbf{A}\mathbf{y} + \mathbf{b}\|_2^2$. To perform gradient evaluations and IHB, we maintain $A \in \mathbb{R}^{m \times \ell}$, $A^\top A \in \mathbb{R}^{\ell \times \ell}$, and $(A^\top A)^{-1} \in \mathbb{R}^{\ell \times \ell}$ throughout OAVI's execution. If the polynomial g constructed in Line 8 of OAVI is not $(\psi, 1)$ -approximately vanishing, then $\|\mathbf{b}\|_2 > 0$, otherwise $g = u_i$ is a vanishing polynomial, a contradiction. Further, $\mathbf{b}^\top A(A^\top A)^{-1}A^\top \mathbf{b} \neq \|\mathbf{b}\|_2^2$, otherwise u_i is the leading term of a vanishing polynomial: $\text{MSE}(g, X) = f(-(A^\top A)^{-1}A^\top \mathbf{b}) = 0$, again, a contradiction. Finally, we have to update $\mathcal{O} \leftarrow (\mathcal{O} \cup \{u_i\})_\sigma$,

$$A \leftarrow \tilde{A} = (A, \mathbf{b}) \in \mathbb{R}^{m \times (\ell+1)}, A^\top A \leftarrow \tilde{A}^\top \tilde{A} \in \mathbb{R}^{(\ell+1) \times (\ell+1)}, \text{ and } (A^\top A)^{-1} \leftarrow (\tilde{A}^\top \tilde{A})^{-1} \in \mathbb{R}^{(\ell+1) \times (\ell+1)}.$$

Updating A and $A^\top A$ requires $O(m\ell + \ell^2)$ operations and then, updating $(A^\top A)^{-1}$ requires an additional $O(\ell^2)$ operations. We formalize below.

Theorem 4.9 (IHB update costs). *Let $A \in \mathbb{R}^{m \times \ell}$, $A^\top A \in \mathbb{R}^{\ell \times \ell}$, $(A^\top A)^{-1}$, and $\mathbf{b} \in \mathbb{R}^\ell$ be given. In the real number model, in case $\|\mathbf{b}\|_2 > 0$ and $\mathbf{b}^\top A(A^\top A)^{-1}A^\top \mathbf{b} \neq \|\mathbf{b}\|_2^2$,*

$$\tilde{A} = (A, \mathbf{b}) \in \mathbb{R}^{m \times (\ell+1)}, \quad \tilde{A}^\top \tilde{A} \in \mathbb{R}^{(\ell+1) \times (\ell+1)}, \quad \text{and} \quad (\tilde{A}^\top \tilde{A})^{-1} \in \mathbb{R}^{(\ell+1) \times (\ell+1)} \quad (4.3)$$

can be constructed in $O(m\ell + \ell^2)$ elementary operations.

Proof. The proof is presented in Appendix A. □

Algorithm 5: Pearson ordering

Input : $X = \{\mathbf{x}_1, \dots, \mathbf{x}_m\} \subseteq [0, 1]^n$.**Output** : X with features sorted according to Pearson.

-
- 1 $\mathbf{c}_i \leftarrow ((\mathbf{x}_1)_i, \dots, (\mathbf{x}_m)_i)^\top \in [0, 1]^m$ for all $i \in \{1, \dots, n\}$ ▷ Feature columns of X
 - 2 $p_i \leftarrow \sum_{j=1}^n |r_{\mathbf{c}_i \mathbf{c}_j}|$ for all $i \in \{1, \dots, n\}$ ▷ Measure the correlation among the features
 - 3 Sort the features of data set X increasingly with respect to p_i for $i \in \{1, \dots, n\}$
-

The proof of Theorem 4.9 is similar to the proof that the inverse of the Hessian can be updated efficiently in the *Online Newton algorithm* (Hazan et al., 2007). However, in our setting, the updates occur column-wise instead of row-wise. Combined with Theorem 4.1, Theorem 4.9 implies the following improved computational complexity of OAVI-IHB compared to the computational complexity of BPCGAVI established in Corollary 4.8.

Corollary 4.10 (Computational complexity of OAVI-IHB). *Let $X = \{\mathbf{y}_1, \dots, \mathbf{x}_m\} \subseteq [0, 1]^n$, $\psi \geq 0$, and $(\mathcal{G}, \mathcal{O}) = \text{OAVI-IHB}(X, \psi)$. In the real number model, the time and space complexities of OAVI-IHB are $O((|\mathcal{G}| + |\mathcal{O}|)^2 m + (|\mathcal{G}| + |\mathcal{O}|)^3)$ and $O((|\mathcal{G}| + |\mathcal{O}|)m + (|\mathcal{G}| + |\mathcal{O}|)^2)$, respectively.*⁸

The numerical results in Figure 3 indicate that CGAVI-IHB is always faster than BPCGAVI and that BPCGAVI-WIHB is always faster than BPCGAVI. In practice, we thus suggest using IHB or WIHB, depending on whether it is important that generators are sparse.

4.5 Discussion

In this section, for a data set $X = \{\mathbf{x}_1, \dots, \mathbf{x}_m\} \subseteq [0, 1]^n$, we proved that the computational complexities of OAVI and ABM are linear in m , polynomial in $|\mathcal{G}| + |\mathcal{O}|$, and, thus, polynomial in n . We also illustrated that improvements in solver speed lead to improvements in training time for OAVI. Finally, we explained how to exploit the fact that OAVI solves a series of optimization problems that differ by very little. We introduced IHB and WIHB, the former leading to massive speed-ups in running time for OAVI and the latter leading to a substantial speed-up in running time while preserving the sparsity-inducing property of Frank-Wolfe algorithms. Overall, the results of this section address the scalability issues of OAVI (and ABM) and support the use of CGAVI-IHB and BPCGAVI-WIHB as feature transformation techniques for large-scale data sets.

5. Data-driven term ordering

As already discussed in Section 1.2, there exist monomial-aware and monomial-agnostic approaches for constructing generators of the ψ -approximate vanishing ideal of a data set $X = \{\mathbf{x}_1, \dots, \mathbf{x}_m\} \subseteq [0, 1]^n$. A previously criticized aspect of monomial-aware approaches such as OAVI is that their output depends on the order in which the features of the data set are arranged (Livni et al., 2013). In this section, we propose a simple fix to this disadvantage of monomial-aware approaches.

We propose to address the issue that the output of OAVI depends on the order of the features in the data set using the *Pearson correlation coefficient* (Benesty et al., 2009).

Definition 5.1 (Pearson correlation coefficient). Given two vectors $\mathbf{a} = (a_1, \dots, a_n)^\top \in \mathbb{R}^n$ and $\mathbf{b} = (b_1, \dots, b_n) \in \mathbb{R}^n$, the *Pearson correlation coefficient* is defined as

$$r_{\mathbf{ab}} = \frac{\sum_{i=1}^n (a_i - \bar{a})(b_i - \bar{b})}{\sqrt{\sum_{i=1}^n (a_i - \bar{a})^2} \sqrt{\sum_{i=1}^n (b_i - \bar{b})^2}},$$

where \bar{a} , \bar{b} are the averages of \mathbf{a} and \mathbf{b} , respectively.

The Pearson correlation coefficient measures linear dependence between two vectors \mathbf{a} and \mathbf{b} and takes absolute value 1 if a linear equation describes the relationship between vector \mathbf{a} and \mathbf{b} perfectly.

⁸. In case OAVI is run with (CCOP), we assume that $\tau \geq 2$ is chosen large enough to guarantee that (INF) never holds.

Table 1: Comparison of test set error in percent for CGAVI-IHB+SVM on several data sets with the Pearson and reverse Pearson ordering of the features of the data set. The results are averaged over ten random 60%/40% train/test partitions and the best results in each category are in bold.

CGAVI+SVM with ordering	Data sets					
	bank	credit	htru	seeds	skin	spam
Pearson	0.00	17.99	2.06	4.29	0.23	6.68
Reverse Pearson	0.00	18.02	2.07	4.29	0.16	6.53

5.1 Algorithm overview

To make monomial-aware algorithms such as OAVI and ABM data-driven, we suggest to order the features of the data using the Pearson correlation coefficient. We refer to the procedure as *Pearson ordering* and present it in Algorithm 5: In Line 1, we consider the column vectors corresponding to the features $i \in \{1, \dots, n\}$ of data set $X = \{\mathbf{x}_1, \dots, \mathbf{x}_m\} \subseteq [0, 1]^n$, a.k.a. the feature columns $\mathbf{c}_i = ((\mathbf{x}_1)_i, \dots, (\mathbf{x}_m)_i)^\top \in [0, 1]^m$ for all $i \in \{1, \dots, n\}$. Then, in Line 2, we compute the absolute Pearson correlations among the features, $p_i = \sum_{j=1}^n |r_{\mathbf{c}_i \mathbf{c}_j}|$ for all $i \in \{1, \dots, n\}$. Finally, in Line 3, we sort the data set X such that its columns are sorted increasingly with respect to the p_i 's. The idea behind first selecting features for which p_i is small is to force OAVI to first consider features that are less linearly correlated with other features.

After ordering the features with Algorithm 5, we then apply OAVI and the output of OAVI remains the same, even if the features of the data set are permuted before applying Algorithm 5. To sort the features of the data set, various alternatives to Algorithm 5 are imaginable. However, as we illustrate in Table 1, the specific ordering of the features seems to have little to no impact on the performance of OAVI. Using the same experimental set-up as in Section 6.2, we compare the classification error on the test set of CGAVI-IHB+SVM with the Pearson ordering to the classification error on the test set of CGAVI-IHB+SVM with the reverse Pearson ordering, which is identical to the Pearson ordering except that the columns are sorted decreasingly with respect to the p_i 's. The results indicate that the specific choice of ordering has little impact on the classification error on the test set.

5.2 Discussion

In this section, we explained how to make monomial-aware algorithms for generator construction of the approximate vanishing ideal fully data-driven using the Pearson correlation coefficient. Furthermore, in the numerical experiment in Table 1, the choice of column ordering for the data set X has little impact on the practical performance of OAVI+SVM. Thus, in this paper, unless noted otherwise, the features of the data are sorted with Algorithm 5 before running monomial-aware algorithms such as OAVI or ABM. Finally, we remark that Algorithm 5 does not always define a unique ordering of the features of the data set. However, when the data set is noisy and has at least three features, the probability that the ordering of the features created via Algorithm 5 is not well-defined is 0.

6. Numerical experiments

In this section, we compare the performance of OAVI as a preprocessing technique for a subsequently applied linear kernel SVM to related approaches.

6.1 General set-up

The general set-up for the numerical experiments outlined here also applies to the smaller experiments that appear throughout the paper.

Table 2: The data sets are retrieved from the UCI Machine Learning Repository (Dua and Graff, 2017). All data sets are binary classification data sets, except for seeds, which is made up of three classes. Each row contains the data set used, its full name and additional references, the number of samples, and the number of features.

Data set	Full name	# samples	# features
bank	banknote authentication	1372	4
credit	default of credit cards (Yeh and Lien, 2009)	30000	22
htru2	HTRU2 (Lyon et al., 2016)	17,898	8
seeds	seeds	210	7
skin	skin (Bhatt and Dhall, 2010)	245,057	3
spam	spambase	4601	57
synthetic	synthetic, see Appendix C	2,000,000	3

Implementation. The numerical experiments are implemented in PYTHON and performed on an NVIDIA GeForce RTX 2080 GPU with 8GB RAM and an Intel Core i7-9700K CPU at 3.60GHz with 64 GB RAM. Our code is publicly available on [GitHub](#).

For all monomial-aware algorithms, unless noted otherwise, we use the Pearson ordering as outlined in Algorithm 5 to order the features of the data sets.

OAVI: We implement OAVI as presented in Algorithm 1. We implement oracles CG, PCG, BPCG, and AGD, and refer to the resulting algorithms as CGAVI, PCGAVI, BPCGAVI, and AGDAVI, respectively. All solvers are run up to accuracy $\varepsilon = 0.01 \cdot \psi$ or up to 10,000 iterations. Solvers are terminated early when not enough progress is made, when the coefficient vector of a generator is constructed, or if we have a guarantee that no coefficient vector of an approximately vanishing polynomial can be constructed with the solver. Whenever OAVI is run with a Frank-Wolfe variant, we replace the optimization problem in Line 7 of OAVI with (CCOP) with $\tau = 1000$. If OAVI is implemented with WIHB or IHB, we refer to the algorithm as OAVI-WIHB or OAVI-IHB, respectively.

ABM: We implement ABM as presented in Limbeck (2013) with the modification that instead of applying the *Singular Value Decomposition* (SVD) to the matrix corresponding to $A = \mathcal{O}(X)$ in OAVI, we apply the SVD to $A^\top A$ in case this leads to a faster training time.

VCA: We implement VCA as presented in Livni et al. (2013) with the modification that instead of applying the SVD to the matrix corresponding to $A = \mathcal{O}(X)$ in OAVI, we apply the SVD to $A^\top A$ in case this leads to a faster training time.

SVM: We implement a polynomial kernel SVM with one-versus-rest approach using the SCIKIT-LEARN software package (Pedregosa et al., 2011). We run the polynomial kernel SVM with ℓ_2 -regularization up to tolerance $1e-3$ or for up to 10,000 iterations.

We use OAVI, ABM, and VCA as preprocessing techniques for a subsequently applied linear kernel SVM as discussed in Section 3.2 and refer to the combined approaches as OAVI+SVM, ABM+SVM, and VCA+SVM, respectively. The subsequently applied linear kernel SVM is implemented using the SCIKIT-LEARN software package, is run with ℓ_1 -penalized squared hinge loss up to tolerance $1e-4$ or for up to 10,000 iterations.

Hyperparameters. For OAVI+SVM, ABM+SVM, and VCA+SVM, the hyperparameters are the vanishing tolerance ψ and the ℓ_1 -regularization coefficient of the linear kernel SVM. For the polynomial kernel SVM, the hyperparameters are the degree and the ℓ_2 -regularization coefficient.

Data sets. The data sets are retrieved from the UCI Machine Learning Repository (Dua and Graff, 2017). An overview of the data sets is given in Table 2. We preprocess each data set with min-max feature scaling after which all data sets are in the range $[0, 1]$.

Table 3: Comparison of test set error in percent, hyperparameter optimization time in seconds, and test time in seconds for CGAVI-IHB+SVM, AGDAVI-IHB+SVM, BPCGAVI-WIHB+SVM, ABM+SVM, VCA+SVM, and polynomial kernel SVM. For the generator-constructing approaches, we also compare the magnitude of $|\mathcal{G}| + |\mathcal{O}|$, the average degree of the constructed generators, and (SPAR). The results are averaged over ten random 60%/40% train/test partitions and the best results in each category are in bold. (For the average degree, we print the highest average degree in bold, even though having high average degree is not necessarily better than having low average degree.)

Algorithms		Data sets					
		bank	credit	htru	seeds	skin	spam
Error test	CGAVI-IHB+SVM	0.00	17.99	2.06	4.29	0.23	6.68
	AGDAVI-IHB+SVM	0.00	17.99	2.06	4.29	0.23	6.68
	BPCGAVI-WIHB+SVM	0.00	18.02	2.05	5.60	0.34	6.72
	ABM+SVM	0.07	18.35	2.09	4.88	0.25	6.55
	VCA+SVM	0.16	19.85	2.11	5.48	0.24	7.15
	SVM	0.00	18.35	2.08	4.76	3.04	7.13
Time hyper.	CGAVI-IHB+SVM	3.1e+00	1.6e+02	3.1e+01	5.5e+00	9.1e+01	1.1e+02
	AGDAVI-IHB+SVM	6.1e+00	1.9e+02	3.5e+01	9.6e+00	9.4e+01	2.1e+02
	BPCGAVI-WIHB+SVM	1.3e+03	4.5e+03	8.2e+02	1.4e+03	7.1e+02	5.2e+02
	ABM+SVM	1.8e+00	1.5e+02	3.0e+01	3.7e+00	5.7e+01	1.8e+02
	VCA+SVM	1.3e+00	2.7e+01	7.2e+00	6.4e+00	1.5e+01	8.2e+01
	SVM	8.4e-02	1.0e+02	5.0e+00	3.7e-02	8.5e+02	2.9e+00
Time test	CGAVI-IHB+SVM	1.5e-03	4.0e-03	1.9e-03	1.8e-03	8.8e-03	3.9e-03
	AGDAVI-IHB+SVM	1.5e-03	4.0e-03	1.9e-03	1.7e-03	8.5e-03	4.e-03
	BPCGAVI-WIHB+SVM	1.6e-03	4.7e-03	2.7e-03	1.8e-03	9.3e-03	4.3e-03
	ABM+SVM	1.5e-03	3.2e-03	1.6e-03	1.7e-03	9.1e-03	2.8e-03
	VCA+SVM	1.0e-03	3.2e-03	1.5e-03	2.7e-03	7.5e-03	7.1e-03
	SVM	3.8e-04	1.7e+00	6.7e-02	2.4e-04	1.2e+01	2.6e-02
$ \mathcal{G} + \mathcal{O} $	CGAVI-IHB+SVM	28.80	85.70	31.80	46.10	24.00	715.30
	AGDAVI-IHB+SVM	28.80	85.70	31.80	46.10	24.00	715.30
	BPCGAVI-WIHB+SVM	31.80	110.90	60.80	47.20	28.50	741.50
	ABM+SVM	25.80	51.40	26.30	44.90	24.00	422.60
	VCA+SVM	23.80	49.80	19.00	181.00	12.40	1766.40
Degree	CGAVI-IHB+SVM	2.09	1.60	1.60	1.60	2.88	1.38
	AGDAVI-IHB+SVM	2.09	1.60	1.60	1.60	2.88	1.38
	BPCGAVI-WIHB+SVM	2.16	1.52	1.98	1.63	3.10	1.53
	ABM+SVM	1.99	1.10	1.26	1.59	2.88	1.24
	VCA+SVM	1.60	1.12	1.12	2.20	1.47	1.72
(SPAR)	CGAVI-IHB+SVM	0.00	0.00	0.00	0.00	0.00	0.01
	AGDAVI-IHB+SVM	0.00	0.00	0.00	0.00	0.00	0.01
	BPCGAVI-WIHB+SVM	0.41	0.70	0.64	0.40	0.23	0.63
	ABM+SVM	0.00	0.00	0.00	0.00	0.00	0.01
	VCA+SVM	0.00	0.00	0.00	0.00	0.00	0.00

6.2 Experiment: performance

We compare the performance of CGAVI-IHB+SVM, BPCGAVI-WIHB+SVM, AGDAVI-IHB+SVM, ABM+SVM, and VCA+SVM and polynomial kernel SVM on the bank, credit, htru, seeds, skin, and spam data sets.

6.2.1 SET-UP.

For several classification data sets, we apply CGAVI-IHB, BPCGAVI-WIHB, AGDAVI-IHB, ABM, and VCA+SVM and polynomial kernel SVM. All results are averaged over ten random 60%/40% train/test partitions. We first tune the hyperparameters of the algorithms on the training data using three-fold cross-validation. Then, for all methods, we retrain on the entire training data set using the best combination of hyperparameters and evaluate the classification error on the test set, the hyperparameter optimization time, and the test time (the times to evaluate the methods on new data). For the generator-constructing methods, we also compare $|\mathcal{G}| + |\mathcal{O}|$, where $|\mathcal{G}| = \sum_i |\mathcal{G}^i|$, $|\mathcal{O}| = \sum_i |\mathcal{O}^i|$, and $(\mathcal{G}^i, \mathcal{O}^i)$ is the output of applying a generator-constructing algorithm to samples belonging to class i . Furthermore, for the generator-constructing methods, we also compare the average degree of the constructed generators. Finally, for generator-constructing methods, we compare the *sparsity of the feature transformation* $\mathcal{G} = \bigcup_i \mathcal{G}^i$, which is defined as

$$\text{SPAR}(\mathcal{G}) = \frac{\sum_{g \in \mathcal{G}} g_z}{\sum_{g \in \mathcal{G}} g_e} \in [0, 1], \quad (\text{SPAR})$$

where for a polynomial $g = \sum_{j=1}^k c_j t_j + t$, $g_e = k$ and $g_z = |\{c_j = 0 \mid j \in \{1, \dots, k\}\}|$, that is, g_e is the number of non-leading-term coefficient vector entries of g and g_z is the number of zero entries in the coefficient vector of g . Then, the sparser the feature transformation, the larger $\text{SPAR}(\mathcal{G})$.

6.2.2 RESULTS.

The results are presented in Table 3.

Test set classification error. Overall, OAVI admits excellent classification error on the test set: CGAVI-IHB+SVM and AGDAVI-IHB+SVM achieve the best test set classification error on two thirds of the data sets and the second best test set classification error on the remaining two data sets. The test set classification error of BPCGAVI-WIHB+SVM is often only slightly worse than that of CGAVI-IHB+SVM and AGDAVI-IHB+SVM, except for seeds, where BPCGAVI-WIHB+SVM admits the worst classification error on the test set. ABM+SVM, VCA+SVM, and polynomial kernel SVM admit classification errors on the test set that are generally worse than those of the approaches based on OAVI. Since the polynomial kernel SVM is only run for up to 10,000 iterations, the algorithm cannot set up the classification boundary for a data set of size 245,057 and the test set classification error for skin is multiple orders of magnitude larger than the test set classification error of the generator-constructing approaches.

Hyperparameter optimization time. The hyperparameter optimization times for the generator-constructing approaches except for BPCGAVI-WIHB+SVM are of a similar order of magnitude, with ABM+SVM and VCA+SVM being on the faster end. Note that the hyperparameter optimization time of BPCGAVI-WIHB+SVM can be several orders of magnitude greater than the hyperparameter optimization times of CGAVI-IHB+SVM and AGDAVI-IHB+SVM due to foregoing IHB in favor of WIHB. Since the training time of polynomial kernel SVM scales superlinearly in m , for the skin data set, the hyperparameter training for the polynomial kernel SVM is the slowest. For smaller data sets, the polynomial kernel SVM is often multiple orders of magnitude faster than the other algorithms.

Test time. The test set evaluation times of the generator-constructing algorithms are similar and fast. For the larger data sets, credit, htru, skin, and spam, the test time of the polynomial kernel SVM is up to several orders of magnitudes slower than that of the generator-constructing algorithms.

The magnitude of $|\mathcal{G}| + |\mathcal{O}|$. For data sets with few features n , the magnitude of $|\mathcal{G}| + |\mathcal{O}|$ is often the smallest for VCA+SVM. However, for spam, a data set with $n = 57$, as already pointed out by Kera and Hasegawa (2019) as the spurious vanishing problem, we observe VCA's tendency to create unnecessary generators. Note that $|\mathcal{G}| + |\mathcal{O}|$ is always smaller for ABM+SVM than for the OAVI-based algorithms. Finally, $|\mathcal{G}| + |\mathcal{O}|$ is always smaller for CGAVI-IHB+SVM and AGDAVI-IHB+SVM than for BPCGAVI-WIHB+SVM.

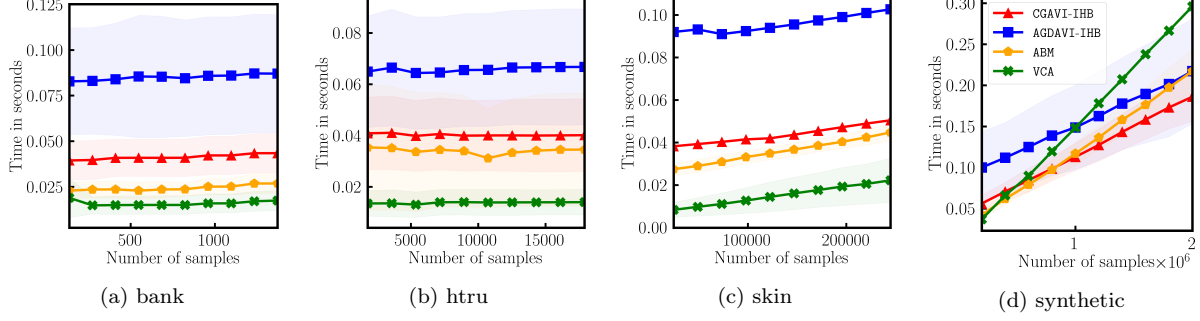


Figure 4: Comparison of the training times of CGAVI-IHB, BPCGAVI-WIHB, AGDAVI-IHB, ABM, and VCA for a varying number of training samples for the bank, htru, skin, and synthetic data sets. The results are averaged over 10 runs and standard deviations are shaded. For small data sets, ABM and VCA are faster than OAVI, but for synthetic, the training times of ABM and VCA scale worse with increasing number of samples than OAVI’s training time.

Average degree. Generally, the average degree of generators constructed by OAVI-based algorithms is higher than the average degree of generators constructed by ABM+SVM or VCA+SVM. On seeds and spam, the two data sets for which $|\mathcal{G}| + |\mathcal{O}|$ is large for VCA+SVM, the average degree of generators constructed by VCA+SVM is the largest.

Sparsity. The feature transformation constructed by BPCGAVI-WIHB+SVM tends to be highly sparse, whereas none of the other algorithms produce feature transformations that exhibit significant sparsity.

Similarity between CGAVI-IHB+SVM and AGDAVI-IHB+SVM. The ℓ_1 -norms of coefficient vectors of generators constructed with CGAVI-IHB+SVM are smaller than $\tau = 1000$. Thus, the outputs and classification errors on the test set of CGAVI-IHB and AGDAVI-IHB are identical. AGDAVI-IHB+SVM is slower than CGAVI-IHB+SVM due to the fact that AGD cannot use the Frank-Wolfe gap as an early termination criterion.

OA VI+SVM better captures non-linear features than ABM+SVM. We observe that the average degree of generators constructed by the OAVI-based approaches is lower than the average degree of generators constructed by ABM+SVM, $|\mathcal{G}| + |\mathcal{O}|$ is always smaller for ABM+SVM than for the OAVI-based algorithms, and ABM+SVM generally admits worse test set classification error than the OAVI-based approaches. This indicates that OAVI-based approaches are better at capturing non-linear features in the data set.

6.3 Experiment: training time

We compare the training times of OAVI, ABM, and VCA for various data sets.

6.3.1 SET-UP.

On at most 10,000 samples of the data set, we tune the hyperparameters of generator-constructing algorithms OAVI, ABM, and VCA and a subsequently applied linear kernel SVM using three-fold cross-validation. Then, using the determined hyperparameters, we run only the generator-constructing algorithms on subsets of the full data set of varying sizes and plot the training times. The results are averaged over 10 runs and standard deviations are shaded. Note that the training times correspond to the times required to run the algorithms once for each class. The compared algorithms are CGAVI-IHB, AGD-IHB, ABM, and VCA and the data sets are bank, htru, skin, and synthetic.

6.3.2 RESULTS.

The results are presented in Figure 4. For small data sets, we observe that **ABM** and **VCA** are faster than **OAVI**. However, when the number of samples in the data set is large, as in the synthetic data set, **OAVI** can be trained faster than **ABM** and **VCA**. **AGDAVI-IHB** is slower than **CGAVI-IHB** because **AGD** cannot use the Frank-Wolfe gap as an early termination criterion.

7. Discussion

We provided a new analysis of the computational complexity of **OAVI**, proving that **OAVI**'s computational complexity depends only linearly on the number of samples in the data set $X = \{\mathbf{x}_1, \dots, \mathbf{x}_m\} \subseteq [0, 1]^n$, an observation that extends to **ABM**. We thus proved that generator-constructing algorithms are scalable techniques to transform the features of data for easier classification with, for example, a linear kernel **SVM**. We supported this theoretical analysis with practical experiments in which we quickly trained **OAVI**, **ABM**, and **VCA** on data sets of up to two million samples. Furthermore, we explored how improving convex solvers leads to improvements in **OAVI**: Replacing **PCG** with the faster **BPCG** leads to a speed-up of **OAVI**. Our final contribution to the scalability of **OAVI** was the introduction of Inverse Hessian Boosting (**IHB**): **OAVI** solves a series of quadratic convex optimization problems that differ only by very little, a fact that we exploited to efficiently update the inverse of the Hessian matrix. Hyperparameter tuning of **OAVI** is sped up by multiple orders of magnitude with **IHB**, which makes **OAVI** the fastest generator-constructing algorithm for very large data sets. Not only did we bring **OAVI** to scale, but we also addressed the second disadvantage of **OAVI** and monomial-aware generator-constructing algorithms: the fact that these algorithms are not fully data-driven. Using the Pearson correlation coefficient, we proposed a sorting scheme of the features of the data set that guarantees that the output of **OAVI** remains the same, agnostic to the initial order of the features of the data set. Combined with the results proved in [Wirth and Pokutta \(2022\)](#), we highlight two attractive algorithms for generator construction, **CGAVI-IHB** and **BPCG-WIHB**, below:

1. For a data set $X = \{\mathbf{x}_1, \dots, \mathbf{x}_m\} \subseteq [0, 1]^n$, both algorithms construct $(\psi, 1)$ -approximately vanishing generators of the ψ -approximate vanishing ideal with computational complexities that depend only linearly on the number of samples m and polynomially on the number of features n .
2. The generators constructed with the algorithms not only vanish approximately on training data but also on out-sample data.
3. The combined approach of transforming features with **CGAVI-IHB** or **BPCG-WIHB** for a subsequently applied linear kernel **SVM** inherits the generalization bound of the **SVM**.
4. Inverse Hessian Boosting guarantees that **CGAVI-IHB** has excellent training times on large data sets.
5. Weak Inverse Hessian Boosting combines the speed-up of **IHB** with the tendency of **BPCG** to produce sparse generators. This creates a reasonably fast algorithm that produces sparse $(\psi, 1)$ -approximately vanishing generators of the ψ -approximate vanishing ideal.

The numerical experiments highlight that the approach of transforming features with a generator-constructing algorithm for a subsequently applied linear kernel **SVM** achieves better classification error on the test set than polynomial kernel **SVM** with better scaling. We thus suggest using **CGAVI-IHB+SVM** and **BPCG-WIHB+SVM** as robust alternatives for non-linear kernel **SVMs** for large-scale machine learning.

ACKNOWLEDGEMENTS

We would like to thank Gabor Braun for providing us with the main arguments for the proof of the pyramidal width of the ℓ_1 -ball. This research was partially funded by Deutsche Forschungsgemeinschaft (DFG) through the DFG Cluster of Excellence MATH⁺ and JST, ACT-X Grant Number JPMJAX200F, Japan.

References

- Abdi, H. and Williams, L. J. (2010). Principal component analysis. *Wiley interdisciplinary reviews: computational statistics*, 2(4):433–459.
- Bartlett, M. S. (1951). An inverse matrix adjustment arising in discriminant analysis. *The Annals of Mathematical Statistics*, 22(1):107–111.
- Benesty, J., Chen, J., Huang, Y., and Cohen, I. (2009). Pearson correlation coefficient. In *Noise reduction in speech processing*, pages 1–4. Springer.
- Bhatt, R. and Dhall, A. (2010). Skin segmentation dataset. *UCI Machine Learning Repository*.
- Carderera, A., Pokutta, S., Schütte, C., and Weiser, M. (2021). Cindy: conditional gradient-based identification of non-linear dynamics – noise-robust recovery.
- Cox, D., Little, J., and O’Shea, D. (2013). *Ideals, varieties, and algorithms: an introduction to computational algebraic geometry and commutative algebra*. Springer Science & Business Media.
- Dua, D. and Graff, C. (2017). UCI machine learning repository.
- Fassino, C. (2010). Almost vanishing polynomials for sets of limited precision points. *Journal of symbolic computation*, 45(1):19–37.
- Frank, M. and Wolfe, P. (1956). An algorithm for quadratic programming. *Naval research logistics quarterly*, 3(1-2):95–110.
- Globerson, A., Livni, R., and Shalev-Shwartz, S. (2017). Effective semisupervised learning on manifolds. In *Proceedings of the 2017 Conference on Learning Theory*, pages 978–1003. PMLR.
- Guélat, J. and Marcotte, P. (1986). Some comments on Wolfe’s ‘away step’. *Mathematical Programming*, 35(1):110–119.
- Guyon, I. and Elisseeff, A. (2003). An introduction to variable and feature selection. *Journal of Machine Learning Research*, 3(Mar):1157–1182.
- Hazan, E., Agarwal, A., and Kale, S. (2007). Logarithmic regret algorithms for online convex optimization. *Machine Learning*, 69(2):169–192.
- Heldt, D., Kreuzer, M., Pokutta, S., and Poullisse, H. (2009). Approximate computation of zero-dimensional polynomial ideals. *Journal of Symbolic Computation*, 44(11):1566–1591.
- Hou, C., Nie, F., and Tao, D. (2016). Discriminative vanishing component analysis. In *Proceedings of the AAAI Conference on Artificial Intelligence*, pages 1666–1672.
- Iraji, R. and Chitsaz, H. (2017). Principal variety analysis. In *Proceedings of the Conference on Robot Learning*, pages 97–108.
- Kera, H. (2021). Border basis computation with gradient-weighted normalization. *arXiv preprint arXiv:2101.00401*.
- Kera, H. and Hasegawa, Y. (2019). Spurious vanishing problem in approximate vanishing ideal. *IEEE Access*, 7:178961–178976.

- Kera, H. and Hasegawa, Y. (2020). Gradient boosts the approximate vanishing ideal. In *Proceedings of the Thirty-Fourth AAAI Conference on Artificial Intelligence*, number 04, pages 4428–4435.
- Kera, H. and Hasegawa, Y. (2021). Monomial-agnostic computation of vanishing ideals. *arXiv preprint arXiv:2101.00243*.
- Kera, H. and Iba, H. (2016). Vanishing ideal genetic programming. In *2016 IEEE Congress on Evolutionary Computation (CEC)*, pages 5018–5025. IEEE.
- Király, F. J., Kreuzer, M., and Theran, L. (2014). Dual-to-kernel learning with ideals. *arXiv preprint arXiv:1402.0099*.
- Kusiak, A. (2001). Feature transformation methods in data mining. *IEEE Transactions on Electronics packaging manufacturing*, 24(3):214–221.
- Lacoste-Julien, S. and Jaggi, M. (2015). On the global linear convergence of Frank-Wolfe optimization variants. In *Advances in Neural Information Processing Systems*, pages 496–504.
- Levitin, E. S. and Polyak, B. T. (1966). Constrained minimization methods. *USSR Computational mathematics and mathematical physics*, 6(5):1–50.
- Limbeck, J. (2013). Computation of approximate border bases and applications.
- Livni, R., Lehavi, D., Schein, S., Nachliely, H., Shalev-Shwartz, S., and Globerson, A. (2013). Vanishing component analysis. In *Proceedings of the Thirteenth International Conference on Machine Learning*, pages 597–605.
- Lyon, R. J., Stappers, B., Cooper, S., Brooke, J. M., and Knowles, J. D. (2016). Fifty years of pulsar candidate selection: from simple filters to a new principled real-time classification approach. *Monthly Notices of the Royal Astronomical Society*, 459(1):1104–1123.
- Manikandan, G. and Abirami, S. (2021). Feature selection is important: state-of-the-art methods and application domains of feature selection on high-dimensional data. In *Applications in Ubiquitous Computing*, pages 177–196. Springer.
- Mohri, M., Rostamizadeh, A., and Talwalkar, A. (2018). *Foundations of machine learning*. MIT press.
- Möller, H. M. and Buchberger, B. (1982). The construction of multivariate polynomials with preassigned zeros. In *European Computer Algebra Conference*, pages 24–31. Springer.
- Nesterov, Y. (1983). A method for unconstrained convex minimization problem with the rate of convergence $O(1/k^2)$. In *Doklady an ussr*, volume 269, pages 543–547.
- Paul, D., Jain, A., Saha, S., and Mathew, J. (2021). Multi-objective pso based online feature selection for multi-label classification. *Knowledge-Based Systems*, 222:106966.
- Pedregosa, F., Varoquaux, G., Gramfort, A., Michel, V., Thirion, B., Grisel, O., Blondel, M., Prettenhofer, P., Weiss, R., Dubourg, V., et al. (2011). Scikit-learn: Machine learning in python. *Journal of Machine Learning Research*, 12:2825–2830.
- Pena, J. and Rodriguez, D. (2019). Polytope conditioning and linear convergence of the frank-wolfe algorithm. *Mathematics of Operations Research*, 44(1):1–18.
- Pokutta, S., Spiegel, C., and Zimmer, M. (2020). Deep neural network training with Frank-Wolfe. *arXiv preprint arXiv:2010.07243*.
- Sherman, J. and Morrison, W. J. (1950). Adjustment of an inverse matrix corresponding to a change in one element of a given matrix. *The Annals of Mathematical Statistics*, 21(1):124–127.
- Stone, J. V. (2004). Independent component analysis: a tutorial introduction.

- Suykens, J. A. and Vandewalle, J. (1999). Least squares support vector machine classifiers. *Neural processing letters*, 9(3):293–300.
- Tsuji, K., Tanaka, K., and Pokutta, S. (2021). Sparser kernel herding with pairwise conditional gradients without swap steps. *arXiv preprint arXiv:2110.12650*.
- Van Der Maaten, L., Postma, E., Van den Herik, J., et al. (2009). Dimensionality reduction: a comparative. *Journal of Machine Learning Research*, 10(66-71):13.
- Vidal, R., Ma, Y., and Sastry, S. (2005). Generalized principal component analysis (gpca). *IEEE transactions on pattern analysis and machine intelligence*, 27(12):1945–1959.
- Wang, L. and Ohtsuki, T. (2018). Nonlinear blind source separation unifying vanishing component analysis and temporal structure. *IEEE Access*, 6:42837–42850.
- Wirth, E. S. and Pokutta, S. (2022). Conditional gradients for the approximately vanishing ideal. In *Proceedings of the 25th International Conference on Artificial Intelligence and Statistics*, pages 2191–2209. PMLR.
- Yeh, I.-C. and Lien, C.-H. (2009). The comparisons of data mining techniques for the predictive accuracy of probability of default of credit card clients. *Expert systems with applications*, 36(2):2473–2480.
- Zhao, Y.-G. and Song, Z. (2014). Hand posture recognition using approximate vanishing ideal generators. In *2014 IEEE International Conference on Image Processing (ICIP)*, pages 1525–1529. IEEE.

Appendix A. Missing proofs

Proof of Theorem 4.9. Let $B = A^\top A \in \mathbb{R}^{\ell \times \ell}$, $\tilde{B} = \tilde{A}^\top \tilde{A} \in \mathbb{R}^{(\ell+1) \times (\ell+1)}$, $N = B^{-1} \in \mathbb{R}^{\ell \times \ell}$, and $\tilde{N} = \tilde{B}^{-1} = (\tilde{A}^\top \tilde{A})^{-1} \in \mathbb{R}^{(\ell+1) \times (\ell+1)}$. In $O(m\ell)$ operations, we construct $A^\top \mathbf{b} \in \mathbb{R}^\ell$, $\mathbf{b}^\top \mathbf{b} = \|\mathbf{b}\|_2^2 \in \mathbb{R}$, and $\tilde{A} = (A, \mathbf{b}) \in \mathbb{R}^{m \times (\ell+1)}$ and in additional $O(\ell^2)$ operations, we construct

$$\tilde{B} = \tilde{A}^\top \tilde{A} = \begin{pmatrix} B & A^\top \mathbf{b} \\ \mathbf{b}^\top A & \|\mathbf{b}\|_2^2 \end{pmatrix} \in \mathbb{R}^{(\ell+1) \times (\ell+1)}.$$

We next compute $\tilde{N} = \tilde{B}^{-1} = (\tilde{A}^\top \tilde{A})^{-1} \in \mathbb{R}^{(\ell+1) \times (\ell+1)}$ in additional $O(\ell^2)$ operations. We write

$$\tilde{N} = \begin{pmatrix} \tilde{N}_1 & \tilde{\mathbf{n}}_2 \\ \tilde{\mathbf{n}}_2^\top & \tilde{n}_3 \end{pmatrix} \in \mathbb{R}^{(\ell+1) \times (\ell+1)},$$

where $\tilde{N}_1 \in \mathbb{R}^{\ell \times \ell}$, $\tilde{\mathbf{n}}_2 \in \mathbb{R}^\ell$, and $\tilde{n}_3 \in \mathbb{R}$. Then, it has to hold that

$$\tilde{B}\tilde{N} = \begin{pmatrix} B & A^\top \mathbf{b} \\ \mathbf{b}^\top A & \|\mathbf{b}\|_2^2 \end{pmatrix} \begin{pmatrix} \tilde{N}_1 & \tilde{\mathbf{n}}_2 \\ \tilde{\mathbf{n}}_2^\top & \tilde{n}_3 \end{pmatrix} = I \in \mathbb{R}^{(\ell+1) \times (\ell+1)},$$

where I is the identity matrix. Note that $\mathbf{b}^\top A \tilde{\mathbf{n}}_2 + \|\mathbf{b}\|_2^2 \tilde{n}_3 = 1$. Thus,

$$\tilde{n}_3 = \frac{1 - \mathbf{b}^\top A \tilde{\mathbf{n}}_2}{\|\mathbf{b}\|_2^2} \in \mathbb{R}, \quad (\text{A.1})$$

which is well-defined due to the assumption $\|\mathbf{b}\|_2 > 0$. Since $\mathbf{b}^\top A$ is already computed, once $\tilde{\mathbf{n}}_2$ is computed, the computation of \tilde{n}_3 requires only additional $O(\ell)$ operations. Similarly, we have that

$$B\tilde{\mathbf{n}}_2 + A^\top \mathbf{b} \tilde{n}_3 = \mathbf{0} \in \mathbb{R}^\ell. \quad (\text{A.2})$$

Plugging (A.1) into (A.2), we obtain

$$\left(B - \frac{A^\top \mathbf{b} \mathbf{b}^\top A}{\|\mathbf{b}\|_2^2} \right) \tilde{\mathbf{n}}_2 = -\frac{A^\top \mathbf{b}}{\|\mathbf{b}\|_2^2}.$$

Thus,

$$\tilde{\mathbf{n}}_2 = -\left(B - \frac{A^\top \mathbf{b} \mathbf{b}^\top A}{\|\mathbf{b}\|_2^2} \right)^{-1} \frac{A^\top \mathbf{b}}{\|\mathbf{b}\|_2^2}.$$

The existence of $\left(B - \frac{A^\top \mathbf{b} \mathbf{b}^\top A}{\|\mathbf{b}\|_2^2} \right)^{-1}$ follows from the Sherman-Morrison formula (Sherman and Morrison, 1950; Bartlett, 1951) and the assumption that $\mathbf{b}^\top A (A^\top A)^{-1} A^\top \mathbf{b} \neq \|\mathbf{b}\|_2^2$. Then,

$$\tilde{\mathbf{n}}_2 = -\left(B^{-1} + \frac{B^{-1} A^\top \mathbf{b} \mathbf{b}^\top A B^{-1}}{\|\mathbf{b}\|_2^2 - \mathbf{b}^\top A B^{-1} A^\top \mathbf{b}} \right) \frac{A^\top \mathbf{b}}{\|\mathbf{b}\|_2^2},$$

which can be computed using additional $O(\ell^2)$ operations. Finally, we construct \tilde{N}_1 , which is determined by

$$B\tilde{N}_1 + A^\top \mathbf{b} \tilde{n}_2^\top = I \in \mathbb{R}^{\ell \times \ell}.$$

Thus,

$$\tilde{N}_1 = B^{-1} - B^{-1} A^\top \mathbf{b} \tilde{n}_2^\top \in \mathbb{R}^{\ell \times \ell},$$

which can be computed in additional $O(\ell^2)$ operations, since $B^{-1} A^\top \mathbf{b} \in \mathbb{R}^\ell$ is already computed. In summary, we require $O(m\ell + \ell^2)$ elementary operations. Note that even if we do not compute $(\tilde{A}^\top \tilde{A})^{-1}$, we still require $O(m\ell + \ell^2)$ elementary operations. \square

Appendix B. Pyramidal width of the ℓ_1 -ball

Pena and Rodriguez (2019) showed that the pyramidal width ω of the ℓ_1 -ball of radius τ , that is, $P = \{\mathbf{x} \in \mathbb{R}^\ell \mid \|\mathbf{x}\|_1 \leq \tau\} \subseteq \mathbb{R}^\ell$ is given by

$$\omega = \min_{F \in \text{faces}(P), \emptyset \subsetneq F \subsetneq P} \text{dist}(F, \text{conv}(P \setminus F)),$$

where, for a polytope $P \subseteq \mathbb{R}^\ell$, $\text{faces}(P)$ denotes the set of faces of P , for a set $F \subseteq \mathbb{R}^\ell$, $\text{conv}(F)$ is the convex hull of F , and for two disjoint sets $F, G \subseteq \mathbb{R}^\ell$, $\text{dist}(F, G)$ is the Euclidean distance between F and G .

Lemma B.1 (Pyramidal width of the ℓ_1 -ball). *The pyramidal width of the ℓ_1 -ball of radius τ , that is, $P = \{\mathbf{x} \in \mathbb{R}^\ell \mid \|\mathbf{x}\|_1 \leq \tau\} \subseteq \mathbb{R}^\ell$, is lower bounded by $\omega \geq \frac{\tau}{\sqrt{\ell}}$.*

Proof. Let $\mathbf{e}_i \in \mathbb{R}^\ell$ denote the i -th unit vector. Note that a face of $P = \text{conv}\{\pm\tau\mathbf{e}_1, \dots, \pm\tau\mathbf{e}_\ell\} \subseteq \mathbb{R}^\ell$ cannot contain both $\tau\mathbf{e}_i$ and $-\tau\mathbf{e}_i$ for any $i \in \{1, \dots, \ell\}$. Thus, without loss of generality, any non-trivial face of P that is not P itself is of the form

$$F = \text{conv}(\{\tau\mathbf{e}_1, \dots, \tau\mathbf{e}_k\})$$

for some $k \in \{1, \dots, \ell - 1\}$. Then,

$$\text{conv}(P \setminus F) = \text{conv}(\{-\tau\mathbf{e}_1, \dots, -\tau\mathbf{e}_k, \pm\tau\mathbf{e}_{k+1}, \dots, \pm\tau\mathbf{e}_\ell\})$$

and

$$\begin{aligned} \text{dist}(F, \text{conv}(P \setminus F)) &= \min_{\mathbf{u} \in F, \mathbf{v} \in G} \|\mathbf{u} - \mathbf{v}\|_2 \\ &= \sqrt{\sum_{i=1}^k (u_i - v_i)^2 + \sum_{j=k+1}^{\ell} v_j^2} \\ &\geq \sqrt{\sum_{i=1}^k (u_i - v_i)^2} \\ &\geq \sqrt{\sum_{i=1}^k u_i^2} \\ &\geq \sqrt{\frac{\tau^2}{k}} \end{aligned}$$

where the second inequality is due to the fact that $v_i \leq 0 \leq u_i$ for all $i \in \{1, \dots, k\}$. Since $\text{dist}(F, \text{conv}(P \setminus F))$ is minimized for a face that is as large as possible, it follows that $\omega \geq \frac{\tau}{\sqrt{\ell}}$. \square

Appendix C. The synthetic data set

The synthetic data set consists of three features and contains two different classes. The samples \mathbf{x} that belong to the first class are generated such that they satisfy the equation

$$x_1^2 + 0.01x_2 + x_3^2 - 1 = 0$$

and samples that belong to the second class are generated such that they satisfy the equation

$$x_1^2 + x_3^2 - 1.3 = 0.$$

The samples are perturbed by additive Gaussian noise with mean 0 and standard deviation 0.05.